



# The Birkhead and Murta formations—organic geochemistry and organic petrography of Mesozoic fluvio-lacustrine source rocks in the Eromanga Basin, central Australia

J. Röth<sup>1</sup> · A. Baniasad<sup>1</sup> · F. Froidl<sup>1</sup> · J. Ostlender<sup>1</sup> · C. Boreham<sup>2</sup> · L. Hall<sup>2</sup> · R. Littke<sup>1</sup>

Received: 6 June 2021 / Accepted: 14 July 2022 / Published online: 24 August 2022  
© The Author(s) 2022

## Abstract

Due to a historic focus on the underlying Cooper Basin and a growing demand for energy in Australia, a reassessment of the Eromanga Basin in central and eastern Australia is necessary, including a more detailed characterization of its Jurassic-Cretaceous petroleum system elements. The Jurassic Birkhead Formation and the Cretaceous Murta Formation are considered the most important source rocks of the Eromanga Basin. To study the petroleum generation potential of these two formations, a set of 55 rock cores from eight petroleum exploration wells was analysed. The sample set was subject to multiple-organic geochemical and petrographical analyses to evaluate organic richness, hydrocarbon potential (Rock–Eval S1 and S2), maceral composition, thermal maturity (e.g. vitrinite reflectance), and saturated and aromatic biomarker composition. The investigated fluvio-lacustrine siltstones and carbonaceous shales exhibit low to excellent total organic carbon (TOC) content, very low sulphur and low inorganic carbon content. Thermal maturity of both formations is at the onset of the oil window (immature to early mature). The Cretaceous Murta Formation shows good hydrocarbon generation potential and, in part, high production indices, while the Jurassic Birkhead Formation generally shows low kerogen to bitumen conversion and a good to very good hydrocarbon generation potential. Dispersed, rather coarse organic matter of terrigenous origin in fine-grained siliciclastic matrix with well-preserved plant remnants including “cutinite flames” is typical. Liptinite (mainly lamalginite) content is generally higher in the Murta Formation (including the occurrence of *Botryococcus* green algae), while vitrinite is clearly dominant in the Birkhead Formation. The Birkhead solvent extracts exhibit a more heterogeneous distribution of *n*-alkanes with distinct maxima in the long-chain range, whereas shorter-chain *n*-alkanes dominate the Murta extracts. Based on their quality and quantity of incorporated organic matter as well as thermal maturity, the petroleum generation potential of the Murta and Birkhead formations is discussed in detail.

**Keywords** Eromanga Basin · Thermal maturity · Petroleum potential · Fluvio-lacustrine shale · Organic petrography · Organic geochemistry

## Introduction and objectives

The region of the Eromanga Basin (Fig. 1a) where it overlies the older Cooper Basin is a mature petroleum province in central Australia. Recent studies aimed to determine

the ultimate potential of the region, assess unconventional resources (e.g. coal bed methane, shale gas, geothermal) and other overlooked opportunities (Hall et al. 2016, 2019 and references therein). However, the petroleum generation potential and biomarker composition of the Eromanga Basin’s source rocks remain partly undefined in the recent numerical basin models. This study aims to reduce these uncertainties where they relate to what are arguably two of its most prolific source rock units, the Birkhead and Murta formations (Michaelsen and McKirdy 2006) and obtained data complement the input of the most recent and fully integrated numerical basin model of the Cooper-Eromanga basin couplet (Röth and Littke 2022).

✉ J. Röth  
joschka.roeth@rwth-aachen.de

<sup>1</sup> Institute of Geology and Geochemistry of Petroleum and Coal, Energy and Mineral Resources Group (EMR), RWTH Aachen University, Lochnerstr. 4-20, 52056 Aachen, Germany

<sup>2</sup> Australian Government, Geoscience Australia, Canberra, Australia

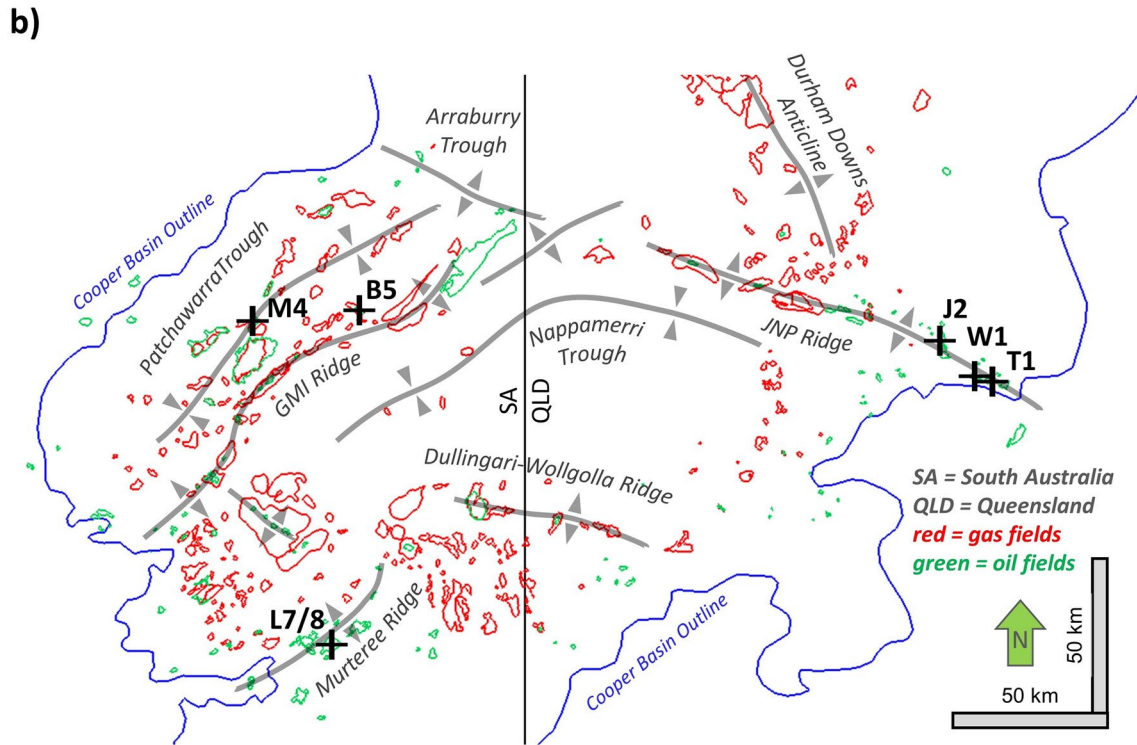
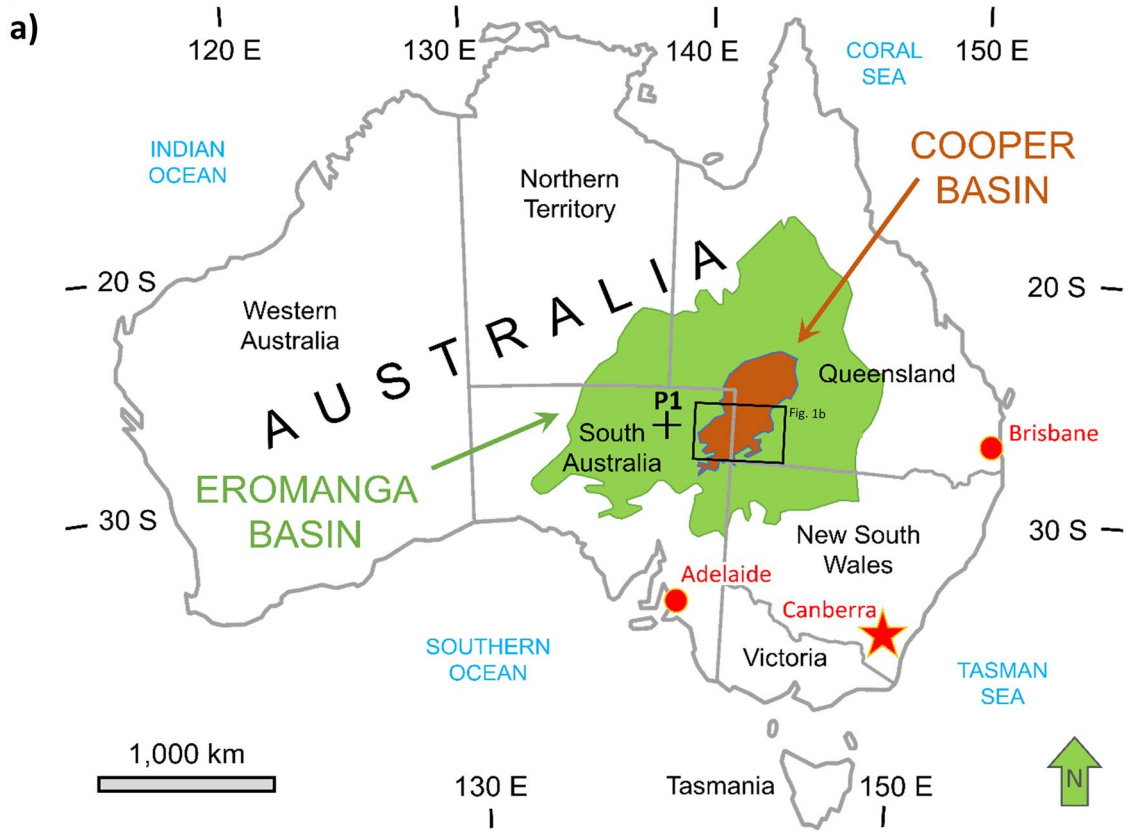


**Fig. 1** Overview of the study area and sample locations. **a** The location of the study area at the border between South Australia and Queensland. The Jurassic-Cretaceous Eromanga Basin unconformable overlies the Late Carboniferous to Triassic Cooper Basin. P1=Poonarunna-1. **b** Sample well locations in the southern Cooper-Eromanga Basin (B5=Bookabourdie-5, M4=Moorari-4, L7/8=Limestone Creek-7/8, J2=Jackson-2, T1=Thungo-1, W1=Winna-1. GMI Ridge=Gidgealpa-Merrimelia-Innamincka Ridge, JNP Ridge=Jackson-Naccowlah-Pepita Ridge. Poonarunna-1 is located outside of this map)

The geologic succession of central-eastern Australia is characterized by several superimposed sedimentary basins: Palaeozoic sequences of the Warburton Basin and sediments of the Late Carboniferous to Triassic Cooper Basin are covered by the Jurassic to Cretaceous Eromanga Basin and the Cainozoic Lake Eyre Basin. Combined, these stacked basins represent Australia's most significant onshore petroleum province. Anticlinal traps, which formed along basement ridges, accommodate most of the associated gas- and oil-fields (Fig. 1b; Hall et al. 2015 and references therein).

The majority of the region's initially discovered hydrocarbons were originally attributed to Permian shales and coals within the Cooper Basin (O'Neil 1998; Boreham et al. 1999; O'Neil and Alexander 2006; Hall et al. 2016 and references therein; APPEA 2020). The source rock potential of the overlying Eromanga Basin needs to be considered as well, notably coals and carbonaceous shales of the Early Jurassic Poolawanna Formation and the Middle Jurassic Birkhead Formation and organic-rich shales and siltstones of the Early Cretaceous Murta Formation (Fig. 2a). The phenomenon of oil mixing became another topic of research, as a result of detailed geochemical and petrographic studies (e.g., Vincent et al. 1985; Michaelsen and McKirdy 1989, 2001, 2006; Kagya 1997; McKirdy et al. 1997; Michaelsen 2002; Deighton et al. 2003; Arouri et al. 2004).

The study area is approximately 127,000km<sup>2</sup> large (as defined by AGBA, 2013, see Fig. 1a). The burial depths and thermal maturity levels of Jurassic and Cretaceous formations were considered too low to be responsible for significant oil generation. However, source rock pods with locally elevated thermal maturity, increased organic matter content, and/or early oil generation from labile organic matter were initially overlooked. Reconstruction of their burial and thermal history (Deighton and Hill 1998; Deighton et al. 2003) provided the first insights into the hydrocarbon generation potential and expulsion of several Eromanga source rocks. However, amounts of paleo-deposition and subsequent erosion due to Late Cretaceous basin inversion are probably more variable than previously assumed and lateral variations of thermal maturity might be underestimated. According to previous research (e.g., Powell et al. 1989; Boulton et al. 1997), the Murta and Birkhead formations are not considered as unconventional

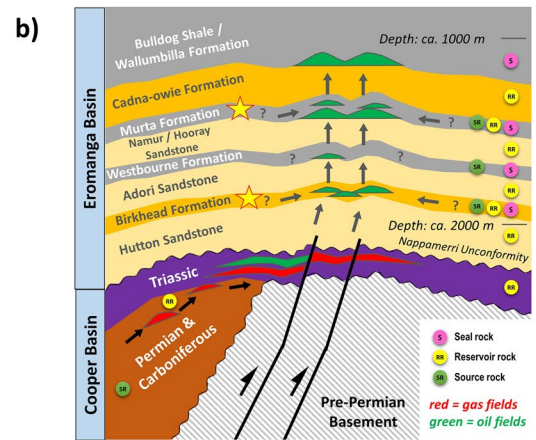
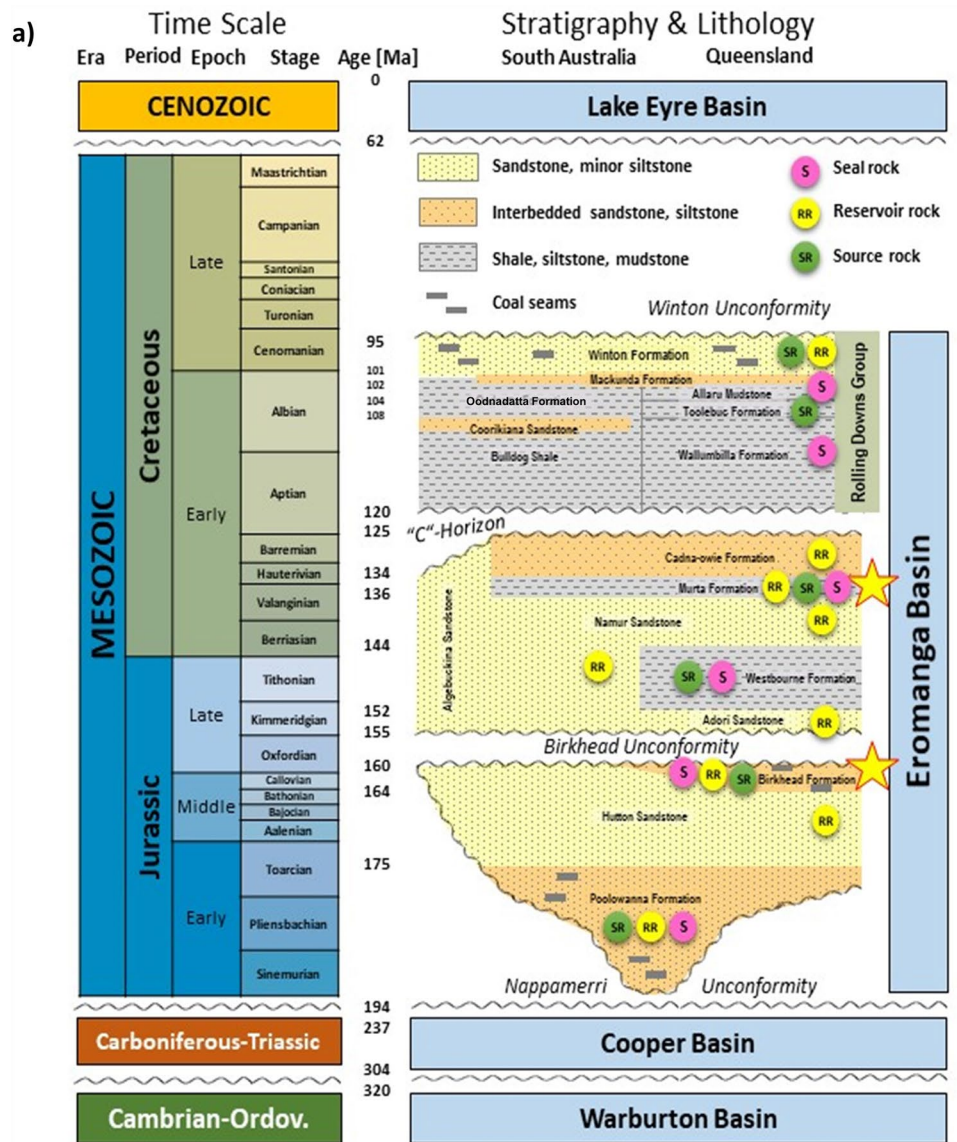
targets (e.g. shale oil), but represent potential source rock intervals that may have contributed to the charge of the Eromanga petroleum system.

A collection of 55 rock cores covering the above-mentioned two formations from eight petroleum exploration wells (Bookabourdie-5 (B5), Jackson-2 (J2), Limestone Creek-7 (L7), Limestone Creek-8 (L8), Moorari-4 (M4), Poonarunna-1 (P1), Thungo-1 (T1), and Winna-1 (W1), see well locations in Fig. 1a and b) was sampled in August 2018 from the core repositories of the South Australia and Queensland state governments (SA Ref. No. 4857, QLD Ref. No. 27146). In this article, a comprehensive study of two important hydrocarbon source rocks in the Eromanga Basin is presented, applying multiple organic geochemical and petrographic methods (elemental analysis, organic petrography, programmed pyrolysis, gas chromatography, and gas chromatography-mass spectrometry)—with data from South Australia and Queensland combined. Oil expulsion from the Birkhead and Murta formations has often been discussed (e.g. Vincent et al. 1985; Michaelsen and McKirdy 1989; Arouri et al. 2004; Hallmann et al. 2006 and references therein), but needs to be confirmed by further studies.

In this study, we have investigated the source rock potential and paleo-depositional environments of the Birkhead and Murta formations within the Eromanga Basin (see Fig. 2b). We evaluated source rock properties such as organic richness (total organic carbon, TOC), hydrocarbon generation potential (Rock-Eval S1 and S2), sulphur content, maceral composition, thermal maturity [ $T_{max}$ , vitrinite reflectance ( $VR_r$  %)] and selected 17 subsamples for analysis of their saturated and aromatic hydrocarbon distributions. We also used the data set to evaluate the paleo-depositional environment based on multiple proxies. Finally, we highlight the similarities and differences of the two source rock formations and formulate theories on their likely respective contributions to oil occurrences in the Eromanga Basin.

Since 2009 exploration has increasingly focussed on unconventional reservoirs (tight gas in the Gidgealpa Group, coal seam gas in the Patchawarra and Toolachee formations, shale gas plays in the Roseneath shale, and mixed lithotype hybrid plays in the Murteree shale (Goldstein et al. 2012; Menpes et al. 2013; Greenstreet and Dello 2015). Although the Cooper and Eromanga basins have the largest datasets of all the onshore sedimentary basins in Australia (Gravestock et al. 1998; Carr et al. 2016), the area is still relatively under-explored (Greenstreet and Dello 2015; Hall et al. 2016). Our detailed analysis of 55 core specimens of the Murta and Birkhead formations from eight exploration wells (four previously unsampled) provides additional data which can be used to estimate the ultimate petroleum potential of the Eromanga Basin.

**Fig. 2** Stratigraphy and petroleum systems of the study area. **a** Chronostratigraphic overview, lithology and petroleum system elements of the study area (modified after AGBA, 2015 and Wainman et al. 2018). **b** Schematic petroleum system of the study area shows possible mixing of hydrocarbons during migration into the anticlinal traps (modified after Bowering and Harrison 1986)



## Geological setting and petroleum system

The system of stacked sedimentary basins in central eastern Australia developed during multiple cycles of westward subduction and periodic crustal accretion along the eastern Australian continental margin. The Palaeozoic to Triassic sedimentary successions of the Warburton, Cooper, Galilee and Bowen basins were blanketed by those of the more widespread Early Jurassic to Late Cretaceous intra-cratonic Great Artesian Basin (GAB). The GAB covers an area of around 1,700,000 km<sup>2</sup> (about one-fifth of Australia) and represents one of the largest artesian aquifer systems in the world (Gravestock et al. 1998; Smerdon et al. 2012; GA 2020a). Besides representing an important source of fresh water for the outback of central-eastern Australia, the strong groundwater flow potentially influenced the migration of oil and gas in the region (Bowering 1982).

Alternating aquiferous sandstones and confining shales and siltstone interbeds of the GAB formed in three major depocentres: the Carpentaria Basin in the north, the Surat Basin in the east and the Eromanga Basin in the centre and in the west (Gravestock et al. 1998). The area of the central and western Eromanga Basin is mainly overlain by the relatively thin (100–200 m) Cainozoic cover of the endorheic Lake Eyre Basin (Draper 2002; Smerdon et al. 2012). The sub-horizontal Eromanga Basin attains its maximum present-day thickness of more than 2 km in the basin depocentre where it directly overlies the Late Carboniferous to Middle Triassic Cooper Basin (Smerdon et al. 2012; Cook et al. 2013; GA 2020b, Fig. 2a).

Following the Triassic Nappamerri Unconformity, the Eromanga Basin formed due to renewed subsidence starting in the Late Triassic. It is stratigraphically divided into four sub-sequences, which are separated by distinct unconformities (Hall et al. 2016):

1. The Late Triassic *Cuddapan Formation* consists of erosional remnants and fluvial deposits and is the precursor of the extensive sedimentary blanket of the Eromanga Basin. Continuous sedimentation was only re-established in the Early Jurassic.
2. The *Early Jurassic to Early Cretaceous fluvio-lacustrine* succession includes the coal-bearing sandstones of the Poolowanna Formation, the widespread Hutton Sandstone and the Birkhead Formation. After a minor interruption (Birkhead Unconformity, see Wainman et al. 2018), the fluvio-lacustrine sub-sequence continues with the Adori Sandstone, Algebuckina Sandstone Westbourne Formation, Namur Sandstone and Murta Formation.
3. The *Early Cretaceous marginal marine to shallow marine* sub-sequence includes the regional sand sheet

of the Cadna-Owie Formation, as well as the Bulldog Shale, the Coorikiana Sandstone and the Oodnadatta Sandstone in South Australia and the Wallumbilla, Toolebuc and Allaru formations in Queensland and finishes with regional Mackunda Formation (Fig. 2a).

4. Above a sharp boundary, the non-marine Late Cretaceous *Winton Formation* comprises the uppermost sub-sequence of the Eromanga Basin.

### The Birkhead Formation

The organic-rich silty and sandy successions of the Birkhead Formation were first defined by Exon (1966) and are the equivalent of the Walloon Coal Measures (or Walloon Formation), which are prevalent in the neighbouring Surat and Clarence-Moreton basins (Reeves 1947). Throughout the central Eromanga Basin the Birkhead Formation overlies the more widespread Middle Jurassic upper Hutton Sandstone and is assigned to the Middle-Late Jurassic PJ4.2—PJ5 palynozones (Paton 1986; Alexander et al. 2006) which correspond to the Callovian to Oxfordian stages (164–160 Ma).

The Birkhead Formation attains a maximum thickness of about 150 m in the Patchawarra and Nappamerri troughs. It predominantly consists of dark grey and brown siltstone, interbedded with mudstone, fine to medium-grained sandstone and thin (<0.3 m), lenticular coal seams. West of the Birdsville Track Ridge the Birkhead Formation laterally interfingers with the Algebuckina Sandstone (Alexander et al. 2006), while the upper boundary is defined by an unconformity against the overlying Namur and Adori sandstones (Draper 2002; AGBA 2015).

The boundary between the Hutton Sandstone and the Birkhead Formation is described as the “top-of-porosity” (Paton 1986; Watts 1987; McIntyre et al. 1989). This petrological change records a provenance shift characterized by the first appearance of labile, lithic fragments sourced from a volcanic arc located along the eastern Australian margin, which superposes the craton-sourced quartz-arenites of the Hutton Sandstone (Watts 1987; Veevers et al. 1991; Boulton 1993; Boulton et al. 1997).

The shift of the depositional environment is also expressed in a facies change from northerly draining low sinuosity braided fluvial (Hutton Sandstone) to easterly flowing high sinuosity meandering deltaic to fluvio-lacustrine environments (Birkhead Formation) (Veevers 1984; Paton 1986; McIntyre et al. 1989; Lanzilli 1999). This sudden drainage reorientation and decrease of energy in the fluvial system was probably caused by intensifying arc activity, increasing influx of volcanogenic sediment and induced isolation from the sea (Lanzilli 1999; Watts 1987; Salomon et al. 1990). During that particular period, the input of organic matter from higher land plants and fresh water algae increased and

its preservation potential likely improved. While the resulting floodplain of “Lake Birkhead” (Mackie and Gumley 1995; Boulton et al. 1997) was fluvial, paleo-depositional conditions may have been temporarily brackish at the connection between the Eromanga Basin and the Carpentaria Basin (Burger 1986). The Birkhead Formation can be subdivided into three units, each measuring about 30 m in thickness (Paton 1986):

- Unit 1 (basal Birkhead Formation): meandering fluvial
- Unit 2 (mid): coal swamp to lacustrine
- Unit 3 (top): meandering to braided fluvial

We identified sand ripples in the investigated rock core material of the Birkhead Formation (see Fig. 3). This observation contradicts calm paleo-depositional environment (Unit 2) and a rough correlation of the evaluated Birkhead Formation samples with either the lower (Unit 1) or the upper (Unit 3) is possible (see Sect. 5.1). The organic matter content of the Birkhead Formation is highly variable, with estimated averages of 2.5 wt. % TOC and a yield of 10.8 kg hydrocarbons/t (Jenkins 1989). While a dominance of “hydrogen-rich” kerogen was determined earlier (Khorasani 1987), more recent studies indicate rather mixed kerogen types with associated hydrogen indices mostly varying between 150 and 500 mgHC/gTOC (McKirdy et al. 1986b; Michaelsen 2002 and references therein; Boreham and Summons 1999; Mahlstedt and Horsfield 2016).

Vitrinite reflectance mapping suggests maturity levels appropriate for oil generation from the Birkhead Formation in the Nappamerri Trough and large areas of south-west Queensland, but expulsion was reported to be very low (Deighton et al. 2003) indicating a relatively late entry to the oil window. Some oil discoveries along the Naccowlah-Jackson Ridge (Queensland) were attributed to Jurassic sources (Vincent et al. 1985). However, large uncertainties remain due to a limited availability of suitable drill core material.

## The Murta Formation

The fluvio-lacustrine successions of the Late Jurassic to Early Cretaceous Namur Sandstone are locally overlain by the fine-grained and organic-rich Murta Formation (Gravestock et al. 1995; Draper 2002; Alexander et al. 2006). This unit interfingers with the Algebuckina Sandstone in the west (South Australia) and the Hooray Sandstone in the east (Queensland) and is covered by the Cadna-owie Formation (Alexander and Sansome 1996). It is assigned to the Early Cretaceous (Neocomian) PK1.2–PK2.1 (Alexander et al. 2006) corresponding to the Valanginian to Hauterivian stages (140–134 Ma).

The Murta Formation has a maximum thickness of about 90 m in the Nappamerri Trough and consists of dark grey

siltstone, interbedded with shale, pale grey very fine to fine-grained sandstone and minor medium and coarse-grained sandstone, locally with reservoir quality (Bowering 1982; Alexander et al. 2006). Fine-grained lacustrine turbidites with recognizable Bouma sequences and slumps indicate slope deposition (Ambrose et al. 1986).

Sedimentation occurred in varied environments including open lacustrine, lacustrine fan delta, distributary channel and lacustrine shoreline under fresh to brackish-marine influence (Mount 1981, 1982; Ambrose et al. 1986; Moore et al. 1986; Zoellner 1988; Wecker 1989; Gorter 1994; Alexander and Sansome 1996). Land plant spores, pollen and the occurrence of *Botryococcus* green algae (e.g. Michaelsen and McKirdy 1989) underline the interpretation of “Lake Murta” (Alexander et al. 2006). Microtidal conditions gave rise to incised channels in which reservoir sands developed (Gorter 1994). A localized, southward-propagating marine transgression from the neighbouring Carpentaria Basin may have occurred during the deposition of the upper Murta Formation (Veevers et al. 1991). From its base to the top the lacustrine Murta Formation can be subdivided into four units (Ambrose et al. 1982, 1986):

- Unit 1: upward-coarsening delta sequence/delta-front
- Unit 2: shallow-water silt and fine sand
- Unit 3: progradational fan sequence/shallowing trend with shoreline bar
- Unit 4: fining-upward, distal, deep water sequence

We interpret the Murta Formation samples investigated herein to have originated from the lower successions (Unit 1 & 2; see Sect. 5.1). The TOC content of the Murta Formation ranges from 0.5 to 2.5 wt. %. Its organic matter originated from mixed sources, giving rise to HI values between 58 and 540 mgHC/gTOC (Michaelsen and McKirdy 1989; Jenkins 1989; Powell et al. 1991; Boreham and Summons 1999; Draper 2002). Thermal maturity measurements indicate that the Murta Formation locally reached the oil window (0.5–0.6 VR<sub>r</sub> %; Powell et al. 1989).

## Petroleum systems

Several episodes of petroleum generation from multiple source rocks are accountable for hydrocarbon fields in the study area (McKirdy et al. 2001; Michaelsen and McKirdy 2001). The Cooper Basin hosts predominantly gas accumulations (including tight gas and coal seam gas), while oil reservoirs are common within the overlying Eromanga Basin (Draper 2002). The composition of the liquid hydrocarbons varies from light oil-condensates to waxy oils with API gravities ranging between 34° and 53° (Boreham and Summons 1999).

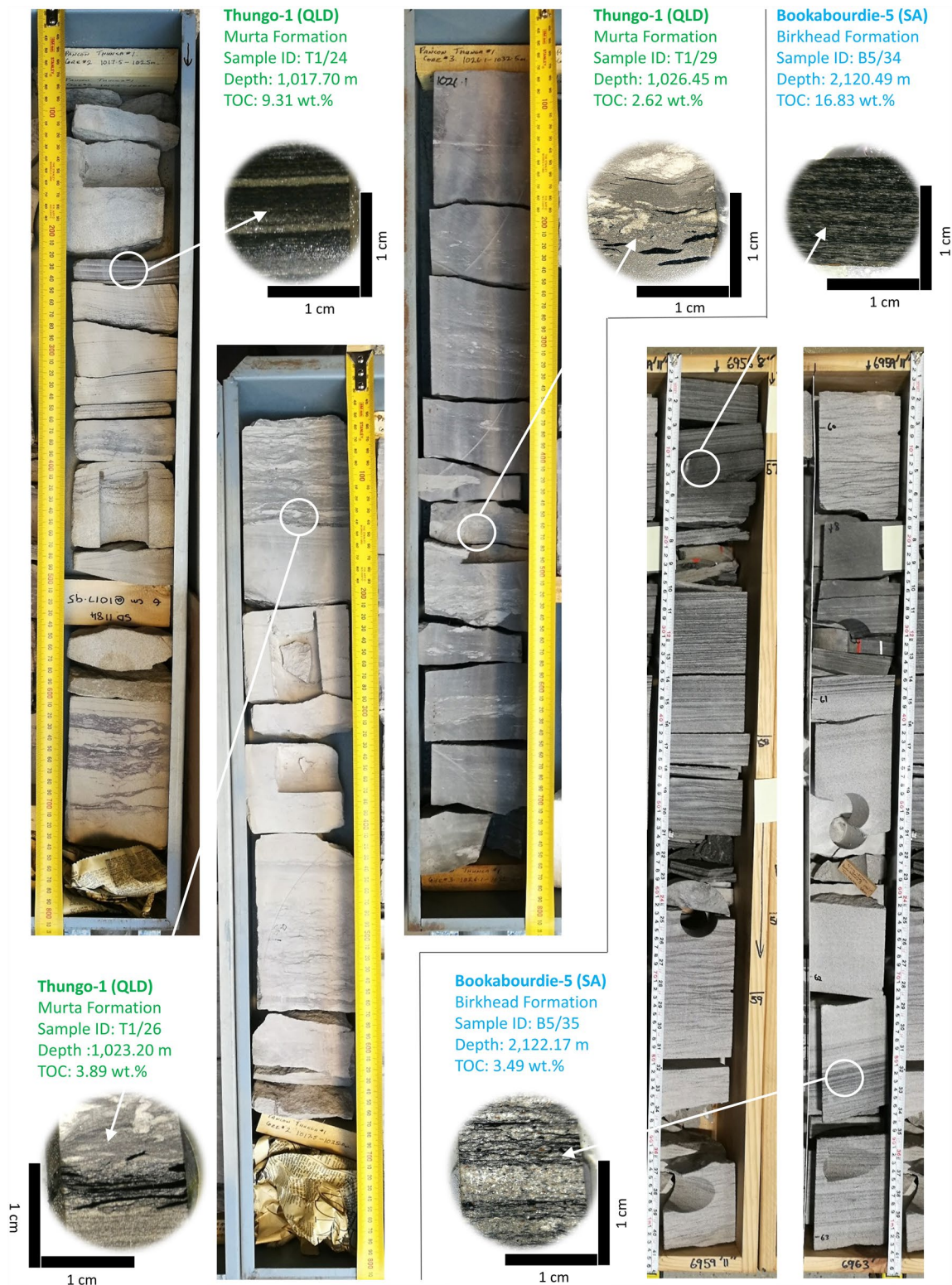


**Fig. 3** Selected cores and samples with remarkable sedimentary features. The sandy siltstones of the Murta Formation at Thungo-1 exhibit interbeds of rhythmic lamination (sample T1/24, varvites) as well as intense bioturbation (sample T1/26), both in combination with

high organic matter content. The laminated and lenticular sandy successions of the Birkhead Formation at Bookabourdie-5 show local cross-bedding and organic-rich interbeds (samples B5/34, B5/35) and exhibit a lower degree of bioturbation

Different source-reservoir couplets occur in both basins. Reservoirs in the Cooper Basin are predominantly charged by Permian sources. Within the Eromanga Basin, Jurassic reservoirs have received a charge from both Jurassic and Permian sources, while the oil found in Cretaceous reservoirs may comprise mixtures of Cretaceous, Jurassic and/or Permian hydrocarbons (Bowering and Harrison 1986; Boreham and Summons 1999; Fig. 2). In addition, there is evidence of minor contributions by pre-Permian marine source rocks to reservoir sandstones in both basins (Hallmann et al. 2006). The bulk of these reservoired hydrocarbons originates from terrigenous organic matter preserved in fluvio-lacustrine shales, siltstones and paludal coals, although quantity and quality are variable (Boreham and Hill 1998; Gravestock et al. 1998; Gray and Draper 2002; Deighton et al. 2003; Jadoon et al. 2016; Hall et al. 2016). Effective oil-prone source rocks have been identified within the Poolowanna, Birkhead, Westbourne and Murta formations of the Eromanga Basin (Draper 2002; Michaelsen and McKirdy 2006). Of these, those in the Birkhead and Murta formations are generally regarded as the most significant (Boreham and Summons 1999).

Together with the Winton Formation, the entire Jurassic to Early Cretaceous formations of the Eromanga Basin (from Poolowanna to Cadna-owie) contains potential reservoirs of varying quality, with those of the Hutton and Hooray sandstones being the most significant (Draper 2002; Deighton et al. 2003). The fine-grained and low-permeable Early Cretaceous marginal marine to shallow marine sub-sequence (from Wallumbilla to Mackunda formation) represents the thickest and most effective regional seal of the study area (Deighton et al. 2003). Major targets in the study area are anticlinal and fault-controlled traps (Draper 2002).

## Materials and analytical methods

The samples were collected in 2018 from the core selection at the regional drill core repositories in Adelaide (Government of South Australia, SA sampling Ref. No. 4857) and Brisbane (Government of Queensland, QLD sampling Ref. No. 27146). Fifty-five core samples of the Murta and Birkhead formations were taken from eight petroleum wells (see Fig. 1 for names and locations, see Table 1 for depth and formation). The particular core intervals were selected based on the availability of sufficient and representative rock material, their proximity to known oil fields, their expected thermal maturity and their estimated organic matter content according to earlier studies (e.g. Michaelsen and McKirdy 1989; Boreham and Summons 1999) and according to the database of Geoscience Australia. Representative fine-grained rock samples (size: quarter core; thickness: varying between 1 and 2 cm) were then sampled. Sandy interbeds

were excluded from the sampling, which resulted in irregular spacing. Additional spot samples were taken from those interbeds where organic particles were recognized macroscopically and where dark brown to black rocks with fine laminations were present. Thus, the sampling was biased towards organic matter-rich and fine-grained lithologies.

At the Institute of Geology and Geochemistry of Petroleum and Coal (RWTH Aachen University, Germany) the core samples were studied using a variety of organic geochemical and organic petrographical methods. From each of the 55 samples, we prepared a powdered sub-sample for bulk geochemical analysis and polished section (see Zieger and Littke 2019) for organic petrographical analysis. We further 17 powdered subsamples were selected for molecular organic geochemistry.

## Organic petrography

The polished sections were embedded in epoxy resin perpendicular to bedding with top and bottom indicated to preserve the original orientation of the laminations and the particles. Vitrinite reflectance ( $VR_r$  %) was measured with a Zeiss Axio Scope.A1 microscope under reflected light with a Zeiss Epiplan-NEOFLUAR 50×/1.0 oil immersion objective and a 10× ocular (total magnification = 500×) equipped with a camera and FOSSIL software (Hilgers Technisches Büro) for data evaluation. Since the measurements were performed on randomly oriented particles the short notation term  $VR_r$  is used (Taylor et al. 1998). Details of the procedure are described in Zieger and Littke (2019).

To determine the thermal maturity of the *in-situ* organic particles, only the autochthonous, low-reflecting vitrinite population was measured, with a preference for large vitrinites. Abundant particles of inertinite and reworked vitrinite were excluded from our analysis.

Qualitative maceral identification was based on Taylor et al. (1998). A selection of 17 subsamples (featuring the highest TOC and including at least two samples from each well) was analysed with a Zeiss Axio Imager.M2m microscope and an Epiplan-NEOFLUAR 50×/1.0 oil objective. Since the TOC contents of most samples are below 10 wt. %, quantitative maceral group counting (500 points, after Taylor et al. 1998) was performed only on the most organic-rich specimen (B5/34, 16.8 wt. % TOC) both in incident white light (for vitrinite and inertinite) and in fluorescence mode for liptinite. For the other samples, maceral group content was estimated based on the evaluation of 20 pictures, each 300 µm in diameter. Each picture was evaluated in reflected and fluorescent light.



**Table 1** Overview of the complete sample set used in this study including lithology

State	Well name/location	MD (m)	Sample ID	Formation	Lithology	Comments
Queensland	Jackson-2 X: 641,029 Y: 6,945,534	1104.59	J2/02	Murta	Sandy siltstone	Appraisal well, oil shows, total depth (TD): 1549.3 m, TD date: 07-MAR-1982
		1105.53	J2/03	Murta	Sandy siltstone	
		1108.87	J2/04	Murta	Fine sandstone	
		1110.33	J2/05*	Murta	Sandy siltstone	
		1111.60	J2/06*	Murta	Sandy siltstone	
		1111.65	J2/07	Murta	Sandy siltstone	
		1116.15	J2/08	Murta	Fine sandstone	
		1116.52	J2/09	Murta	Fine sandstone	
		Winna-1 X: 653,100 Y: 6,932,009	999.91	W1/10	Murta	
	1005.37		W1/11*	Murta	Silty shale	
	1009.91		W1/12	Murta	Sandy siltstone	
	1010.87		W1/13	Murta	Silty shale	
	1010.96		W1/14	Murta	Silty shale	
	1011.05		W1/15	Murta	Silty shale	
	1011.08		W1/16	Murta	Silty shale	
	1011.52		W1/17*	Murta	Sandy siltstone	
	1013.83		W1/18	Murta	Sandy siltstone	
	1016.34		W1/19	Murta	Sandy siltstone	
	1017.34		W1/20	Murta	Sandy siltstone	
	Thungo-1 X: 655,771 Y: 6,931,634	1009.46	T1/21	Murta	Sandy siltstone	Exploration well, oil shows, total depth (TD): 1424.0 m, TD date: 21-MAR-1986
		1010.76	T1/22	Murta	Sandy siltstone	
		1011.35	T1/23	Murta	Sandy siltstone	
		1017.70	T1/24*	Murta	Sandy siltstone	
		1022.41	T1/25	Murta	Sandy siltstone	
		1023.20	T1/26*	Murta	Sandy siltstone	
		1024.97	T1/27	Murta	Fine sandstone	
		1026.40	T1/28	Murta	Silty shale	
		1026.45	T1/29*	Murta	Silty shale	
		1031.16	T1/30	Murta	Sandy siltstone	
		1032.94	T1/31	Murta	Sandy siltstone	
		1033.64	T1/32	Murta	Sandy siltstone	
	South Australia	Bookabourdie-5 X: 448,764 Y: 6,954,111	2120.07	B5/33	Birkhead	Sandy siltstone
2120.49			B5/34*	Birkhead	Sandy siltstone	
2122.17			B5/35*	Birkhead	Fine sandstone	
Moorari-4 X: 414,502 Y: 6,951,619		2155.24	M4/36	Birkhead	Sandy siltstone	Development well, oil/gas, total depth (TD): 2954.1 m, TD date: 15-JAN-1982
		2156.15	M4/37*	Birkhead	Sandy siltstone	
		2159.75	M4/38	Birkhead	Sandy siltstone	
		2160.12	M4/39	Birkhead	Sandy siltstone	
		2160.18	M4/40*	Birkhead	Sandy siltstone	
2160.45		M4/41	Birkhead	Sandy siltstone		
Limestone-Creek-8 X: 440,972 Y: 6,844,654		1199.97	L8/42*	Murta	Sandy siltstone	Development well, oil shows, total depth (TD): 1306.4 m, TD date: 04-MAR-1988
	1200.64	L8/43	Murta	Sandy siltstone		
	1205.45	L8/44*	Murta	Sandy siltstone		

**Table 1** (continued)

State	Well name/location	MD (m)	Sample ID	Formation	Lithology	Comments
	Limestone-Creek-7	1206.00	L7/45*	Murta	Sandy siltstone	Development well, oil shows, total depth (TD): 1303.6 m, TD date: 29-JUL-1987
	X: 440,787	1210.76	L7/46*	Murta	Sandy siltstone	
	Y: 6,845,289	1216.00	L7/47	Murta	Sandy siltstone	
	Poonarunna-1	1584.30	P1/48	Birkhead	Shale	Exploration well, dry, total depth (TD): 1699.3 m, TD date: 06-OCT-1964
	X: 786,875	1587.80	P1/49	Birkhead	Shale	
	Y: 6,910,113	1596.10	P1/50	Birkhead	Shale	
		1601.30	P1/51	Birkhead	Fine sandstone	
		1602.03	P1/52	Birkhead	Fine sandstone	
		1621.11	P1/53	Birkhead	Sandy siltstone	
		1622.78	P1/54	Birkhead	Sandy siltstone	
		1625.07	P1/55*	Birkhead	Sandy siltstone	
		1625.44	P1/56*	Birkhead	Silty shale	

Rock–Eval pyrolysis and petrographic determination of thermal maturity was performed on all samples (results summarized in Table 2). Asterisks indicate samples which underwent molecular organic geochemical analysis due to high TOC (at least two samples per well, see Table 3)

### Bulk organic geochemistry

Total organic carbon, inorganic carbon and sulphur (TOC, TIC and  $T_S$ , expressed as wt. %) were measured on powdered rock samples with an Elementar liqui-TOC II instrument and a LECO S-200 Sulfur Analyser, respectively.

The whole sample set was then analysed with a Vinci Rock–Eval 6 instrument using the cycle of analysis and indices described by Tissot and Welte (1984) and by applying the non-isothermal bulk rock method of Béhar et al. (1984). From the TOC values and the peaks of Rock–Eval S1 (free hydrocarbons) and S2 (thermally generated “cracked” hydrocarbons) the evaluation parameters Hydrogen Index (HI [mg HC/g TOC] =  $S2/TOC \times 100$ ), Genetic Potential (GP [mg HC/g rock] =  $S1 + S2$ ) and Production Index (PI [–] =  $S1/(S1 + S2)$ ) are derived. The evaluation and interpretation of our elemental analysis (TOC, TIC,  $T_S$ ) and the results of the Rock–Eval pyrolysis ( $T_{max}$ , S1, S2, etc.) followed the traditional approaches described by Espitalié et al. (1977), Tissot and Welte (1984), Peters and Cassa (1994), and Law (1999). The resulting bulk geochemical data are listed in Table 2.

### Molecular organic geochemistry

Detailed molecular analysis was performed on subsamples of the two formations (Birkhead,  $n = 6$ ; Murta,  $n = 11$ ) by following standard workflows for organic matter extraction (Guo et al. 2020) and for subsequent fractionation (Schwarzbauer and Jovančićević 2020).

Gas chromatography (GC) with coupled flame ionization detector (GC-FID) and gas chromatography with coupled mass spectrometry (GC–MS) were conducted on aliphatic and aromatic fractions as recently described in detail by Fang et al. (2019).

Compound identifications are based on comparison with reference standards, selected molecular ions, retention properties and elution orders of published gas chromatograms. Separation of co-eluted compounds, e.g.  $C_{27}$   $\alpha\alpha$  20R and  $C_{29}$   $\beta\alpha$  diasteranes 20R was conducted using relative mass-to-charge ratios, i.e.  $m/z$  372 and 400. Biomarker ratios are based on the integration of peak areas derived from specific ion chromatograms. The compounds relevant for this study are listed in supplementary information S3.

### Results

A detailed source rock evaluation includes the determination of organic richness (quantity), kerogen type, maceral composition, molecular signatures (quality) and thermal maturity (Peters and Cassa 1994). The investigated rock samples represent non-marine mudstones, siltstones, fine-grained sandstones and carbonaceous shales. Both studied formations can be macroscopically characterized as fluvio-lacustrine siliciclastics (Fig. 3). Typical features are fine, commonly wavy laminations of interbedded sand, silt and clay, as well as lenticular bedding and bioturbation. In the following, the detailed results of our investigations are summarized (see also Tables 2, 3).

**Table 2** Overview of Rock–Eval pyrolysis results (S1, S2, oil saturation index OSI, production index PI, and hydrogen index HI) sorted after formation and including elemental composition (TOC, TIC, and  $T_S$ ) and vitrinite reflectance (VRr mean, with standard deviations)

Formation	Sample ID	TOC (%)	TIC (%)	$T_S$ (%)	S1 (mg HC/g rock)	S2 (mg HC/g rock)	OSI (mg HC/g TOC)	PI (-)	HI (mg HC/g TOC)	$T_{max}$ (°C)	VRr mean (%)	VRrs (%)
Murta	J2/02	0.86	0.02	0.09	0.05	0.55	5.77	0.08	64	437	0.56	0.052
	J2/03	0.98	0.02	0.10	0.07	0.75	6.95	0.08	76	440	0.56	0.062
	J2/04	2.29	0.02	0.07	0.20	0.99	8.70	0.17	43	433	0.59	0.059
	J2/05*	4.29	0.02	0.07	2.34	1.59	54.40	0.60	37	425	0.63	0.077
	J2/06*	2.86	0.03	0.13	5.16	5.03	180.13	0.51	176	432	0.58	0.071
	J2/07	1.97	0.02	0.11	2.45	3.48	124.47	0.41	176	430	0.53	0.058
	J2/08	1.78	0.02	0.12	0.82	4.78	45.75	0.15	268	437	0.53	0.051
	J2/09	2.25	0.01	0.12	0.91	5.14	40.42	0.15	229	432	0.57	0.072
	W1/10	0.75	0.01	0.11	0.28	0.90	37.76	0.24	120	431	0.55	0.045
	W1/11*	4.57	0.02	0.14	5.31	9.70	116.13	0.35	212	430	0.54	0.034
	W1/12	0.86	0.01	0.09	0.83	1.96	96.12	0.30	228	436	0.54	0.042
	W1/13	1.44	0.01	0.11	0.53	3.13	36.56	0.14	217	437	0.58	0.057
	W1/14	2.15	0.01	0.20	0.40	2.90	18.55	0.12	135	431	0.56	0.052
	W1/15	3.10	0.02	0.17	0.37	2.14	11.92	0.15	69	430	0.58	0.047
	W1/16	1.99	0.02	0.17	0.32	3.09	15.85	0.09	155	434	0.59	0.053
	W1/17*	1.10	0.01	0.11	4.29	2.29	388.75	0.65	208	428	0.56	0.049
	W1/18	2.03	0.26	0.16	1.15	3.96	56.73	0.23	195	436	0.62	0.058
	W1/19	1.38	0.01	0.10	0.53	1.46	38.62	0.27	106	435	0.59	0.068
	W1/20	2.10	0.01	0.11	2.00	3.18	95.25	0.39	152	430	0.60	0.065
	T1/21	1.24	0.01	0.10	1.00	1.88	80.77	0.35	152	437	0.57	0.057
	T1/22	1.91	0.01	0.11	0.86	3.87	45.21	0.18	203	436	0.54	0.038
	T1/23	1.13	0.01	0.08	0.78	1.90	69.23	0.29	168	436	0.56	0.040
	T1/24*	9.31	0.02	0.20	12.94	22.85	139.04	0.36	245	427	0.52	0.047
	T1/25	1.50	0.01	0.08	0.24	1.46	15.89	0.14	97	433	0.63	0.054
	T1/26*	3.89	0.01	0.12	1.56	7.61	40.11	0.17	196	432	0.53	0.035
	T1/27	0.50	3.33	0.05	0.17	0.98	34.44	0.15	196	436	0.55	0.048
	T1/28	1.56	0.01	0.10	0.21	3.38	13.67	0.06	217	437	0.57	0.059
	T1/29*	2.62	0.03	0.12	0.45	5.55	17.23	0.08	212	435	0.59	0.065
	T1/30	1.71	0.01	0.12	0.27	2.66	15.75	0.09	156	432	0.66	0.055
	T1/31	0.98	0.01	0.08	0.10	1.13	10.26	0.08	115	433	0.70	0.084
	T1/32	2.38	0.01	0.11	0.35	6.15	14.67	0.05	258	433	0.58	0.059
	L8/42*	2.71	0.01	0.13	0.29	3.25	10.77	0.08	120	433	0.65	0.065
	L8/43	1.83	0.02	0.10	0.17	1.48	9.10	0.10	81	430	0.73	0.053
	L8/44*	5.86	0.10	0.07	0.86	1.63	14.75	0.35	28	425	0.62	0.080
	L7/45*	2.85	0.05	0.11	0.67	3.40	23.37	0.16	119	431	0.61	0.055
	L7/46*	1.59	0.10	0.07	0.74	1.47	46.60	0.34	92	429	0.56	0.051
	L7/47	1.18	0.02	0.08	0.36	1.56	30.60	0.19	132	429	0.61	0.058

Table 2 (continued)

Formation	Sample ID	TOC (%)	TIC (%)	T <sub>S</sub> (%)	S1 (mg HC/g rock)	S2 (mg HC/g rock)	OSI (mg HC/g TOC)	PI (-)	HI (mg HC/g TOC)	T <sub>max</sub> (°C)	VRr mean (%)	VRrs (%)
Birkhead	B5/33	2.68	0.02	0.10	1.07	6.59	39.91	0.14	246	433	0.57	0.053
	B5/34*	16.83	0.03	0.33	5.49	61.24	32.60	0.08	364	432	0.65	0.045
	B5/35*	3.49	0.02	0.15	0.96	8.09	27.53	0.11	232	433	0.65	0.065
	M4/36	0.98	0.02	0.08	0.43	2.94	43.78	0.13	300	434	0.56	0.048
	M4/37*	3.59	0.02	0.13	1.35	11.51	37.61	0.10	321	427	0.56	0.046
	M4/38	1.87	0.02	0.10	0.66	3.61	35.19	0.15	193	428	0.55	0.035
	M4/39	1.41	0.02	0.08	0.61	2.86	43.28	0.18	203	430	0.58	0.044
	M4/40*	1.93	0.02	0.10	0.51	3.55	26.70	0.13	184	431	0.57	0.054
	M4/41	1.91	0.02	0.11	0.56	3.89	29.20	0.13	203	432	0.55	0.046
	P1/48	1.41	0.05	0.09	0.25	5.76	17.89	0.04	408	436	0.57	0.032
	P1/49	1.85	0.05	0.11	0.39	8.07	20.88	0.05	436	439	0.54	0.043
	P1/50	0.99	0.03	0.10	0.12	3.92	12.08	0.03	396	435	0.63	0.040
	P1/51	2.56	0.03	0.12	0.41	8.27	16.02	0.05	323	437	0.58	0.049
	P1/52	2.66	0.03	0.13	0.45	8.67	16.84	0.05	326	434	0.56	0.051
	P1/53	2.41	0.03	0.13	0.54	7.58	22.22	0.07	315	437	0.51	0.044
	P1/54	2.26	0.03	0.12	0.51	7.07	22.54	0.07	313	436	0.51	0.028
	P1/55*	9.07	0.19	0.19	2.21	33.31	24.33	0.06	367	430	0.61	0.045
	P1/56*	9.24	0.03	0.18	2.74	34.27	29.66	0.07	371	436	0.61	0.036

Samples with asterisk underwent molecular organic geochemical analysis (see Table 3)

## Organic richness and carbonate content

TOC values vary between 0.5 and 16.8% (Table 2). The average values for both formations (Murta, 2.3%; Birkhead, 3.7; see Table 2) should be regarded with caution since the sampling process was focused on the richest beds and was not conducted at a constant interval along the entire thickness of each formation. Further, the analysed core only covers sections of the formations, but not their entire thickness. Seven samples contain less than 1.0% TOC, with most values ranging between 1 and 5%.

Extraordinarily high TOC values were obtained from the visibly carbonaceous samples of the Birkhead Formation (B5/34, 16.8%, P1/55, 9.1%; P1/56, 9.2%) and one sample of the Murta Formation (T1/24, 9.3%).

The measured TIC values fall mainly in the range of 0.01 to 0.05%, with the Murta sample T1/27 yielding an anomalously high value of 3.3%. From their TIC values, the carbonate content of the rock samples can be derived. While most samples do not contain more than 0.4% CaCO<sub>3</sub>, the maximum TIC value corresponds with the minimum TOC and  $T_S$  values (T1/27, TOC = 0.50%,  $T_S$  = 0.05%, TIC = 3.3%) and yields 27.7% CaCO<sub>3</sub>.

## Sulphur content

Total sulphur contents are low between 0.05 and 0.3% (Murta Formation avg.: 0.11%; Birkhead Formation avg.: 0.13%) and show a linear relationship with the TOC content. The minimum  $T_S$  value corresponds with the minimum TOC value (T1/27: TOC = 0.5%,  $T_S$  = 0.05%) and the maxima also correlate (B5/34: TOC = 16.8%,  $T_S$  = 0.3%). The overall  $T_S$  / TOC ratio is around 1:78.

## Rock–Eval pyrolysis

Rock–Eval parameters S1, S2, GP, PI and HI (Table 2) were used to characterize and quantify the hydrocarbon potential of the two formations. HI values are generally higher for the Birkhead Formation (184–436; avg.: 306) than the Murta Formation (64–268; avg.: 153). The obtained data are presented in Table 2 and are discussed in more detail below. Representative Rock–Eval pyrograms are provided in the supplementary information.

## Vitrinite reflectance $VR_r$ and Rock–Eval $T_{max}$

Vitrinite reflectance ( $VR_r$ ) and Rock–Eval  $T_{max}$  are indicators of the level of thermal maturity in rock samples (Hartkopf-Fröder et al. 2015). The relationship between both

parameters is usually linear (see Hackley and Cardott 2016; Yang and Horsfield 2020 for a non-linear correlation). The values of both formations are very similar ranging between 425 and 440 °C  $T_{max}$  (avg. for both: 433 °C) and between 0.5 and 0.7  $VR_r$  %, respectively (Murta Formation avg.: 0.58  $VR_r$  %; Birkhead Formation avg.: 0.57  $VR_r$  %). Representative  $VR_r$  measurements are provided in the supplementary information.

## Organic petrography

Based on examination of the cores and the polished sections, we characterize the samples as carbonaceous sandy siltstones and silty shales (Fig. 4; Table 1). Both formations exhibit laminated sediment structures with varying intensities of bioturbation. Organic matter occurs in various forms—as dispersed organic matter (DOM) in coarse mineral detritus (Fig. 4a, b) or as fine particles in fine-grained siliciclastic matrix (Fig. 4c). Well-preserved plant-remnants are common.

The observed maceral group composition (vitrinite, liptinite, and inertinite) of the examined samples is displayed as a ternary diagram in Fig. 4d. All samples exhibit relatively high amounts of vitrinite and liptinite. While vitrinite is dominant in the Birkhead Formation (vitrinite 63–85%, liptinite 10–37%), the liptinite content is generally higher in the Murta Formation (vitrinite 37–80%, liptinite 20–60%). Inertinite is the least abundant maceral group, although more common in the Birkhead Formation. In Fig. 4d the two formations plot in two largely separate clusters (Murta, liptinite > vitrinite > inertinite; Birkhead, vitrinite > liptinite > inertinite). Three Murta samples (W1/17, T1/26, and T1/27) lie within the Birkhead cluster, having a high vitrinite to liptinite ratio (80:20) and lacking inertinite.

In UV-excited fluorescent mode, we identified cutinite, lamalginitite and telalginitite. While thinner lamalginitite is abundant in the Murta Formation (Fig. 4c), relatively thick laminated fragments occur in the Birkhead Formation. Well-preserved flame-shaped cutinite phytoclasts (Fig. 4a, b) are present in those samples with the highest TOC values (T1/24, Murta; B5/34, Birkhead). While the fluorescence colour of the “cutinite flames” (remnants of leaf cuticle from higher plants) is bright yellow in the Murta Formation (Fig. 4a), it appears as darker orange in the Birkhead Formation (Fig. 4b). This colour change reflects the difference in depth and thermal maturity of the shallower Murta Formation (T1/24,  $VR_r$  = 0.52%) and the deeper Birkhead Formation (B5/34,  $VR_r$  = 0.65%). Sporadic occurrence of bright yellow to light orange fluorescent telalginitite derived from *Botryococcus* algae in the Murta Formation (also observed by Michaelsen and McKirdy 1989) was confirmed in some samples (Fig. 4c).

**Table 3** Results of molecular organic geochemistry sorted after formation and distinguished between GC-FID and GC-MS (see supplementary information S3 for abbreviations)

Formation	Sample ID	GC-MS molecular fractions, ratios and indices													
		Hopanes													
		Pr/Ph <sup>a</sup>	Pr/n-C <sub>17</sub> <sup>b,c</sup>	Ph/n-C <sub>18</sub> <sup>b,c</sup>	n-C <sub>17</sub> /n-C <sub>27</sub> <sup>a</sup>	TAR <sup>d</sup>	OEP <sup>e</sup>	C <sub>19</sub> /C <sub>23</sub> <sup>a</sup>	C <sub>29</sub> /C <sub>30</sub> <sup>f,g</sup>	T <sub>S</sub> /(T <sub>S</sub> +T <sub>M</sub> ) <sup>a</sup>	C <sub>29</sub> T <sub>S</sub> /(C <sub>29</sub> T <sub>S</sub> +C <sub>29</sub> ) <sup>a</sup>	C <sub>30</sub> M/(C <sub>30</sub> +C <sub>30</sub> M) <sup>h</sup>	C <sub>31</sub> 22S/(22S+22R) <sup>h</sup>		
Murta	J2/05	2.55	0.32	0.10	3.99	0.17	1.01	4.38	0.65	0.35	0.20	0.20	0.56		
	J2/06	3.10	0.28	0.10	40.64	0.01	1.12	7.33	0.56	0.31	0.30	0.15	0.51		
	W1/11	2.32	0.32	0.13	20.12	0.02	1.00	13.16	0.61	0.27	0.24	0.18	0.56		
	W1/17	2.50	0.39	0.14	3.62	0.16	1.03	5.46	0.69	0.27	0.21	0.19	0.55		
	T1/24	3.44	0.28	0.09	581.52	0.00	1.08	10.17	0.68	0.26	0.18	0.27	0.54		
	T1/26	6.74	0.34	0.11	65.22	0.01	1.05	5.24	1.03	0.13	0.14	0.30	0.58		
	T1/29	3.62	0.54	0.16	2.12	0.34	1.09	2.26	0.64	0.23	0.19	0.20	0.61		
	L8/42	2.73	0.20	0.06	16.35	0.03	1.19	3.12	0.60	0.11	0.15	0.28	0.57		
	L8/44	1.93	0.18	0.09	2.48	0.19	1.04	2.52	0.58	0.27	0.22	0.23	0.60		
	L7/45	3.26	0.22	0.07	38.33	0.02	1.10	5.35	0.67	0.23	0.21	0.22	0.57		
	L7/46	3.09	0.24	0.07	65.04	0.01	1.07	3.24	0.62	0.29	0.31	0.22	0.46		
	Birkhead	B5/34	5.21	0.84	0.18	1.41	0.57	1.07	13.17	0.60	0.12	0.11	0.13	0.59	
		B5/35	4.55	1.11	0.23	1.26	0.39	1.05	4.94	0.66	0.16	0.15	0.11	0.58	
		M4/37	6.67	1.26	0.21	4.04	0.18	1.04	8.05	0.66	0.25	0.23	0.17	0.60	
		M4/40	9.92	1.40	0.22	0.69	0.85	1.13	3.05	0.50	0.31	0.29	0.16	0.58	
		P1/55	6.02	1.65	0.24	0.31	1.91	1.04	14.87	0.52	0.18	0.16	0.14	0.58	
	P1/56	6.37	1.68	0.24	0.37	1.52	1.04	16.81	0.58	0.21	0.19	0.13	0.58		
Formation	Sample ID	GC-MS molecular fractions, ratios and indices													
		Steranes							Aromatics						
		C <sub>27</sub> (%) <sup>g,i</sup>	C <sub>28</sub> (%) <sup>g,i</sup>	C <sub>29</sub> (%) <sup>g,i</sup>	C <sub>29</sub> ααα / 20S/20S + 20R <sup>i</sup>	C <sub>29</sub> αββ/αββ + ααα <sup>i</sup>	C <sub>29</sub> ααα / 20S/20S + 20R <sup>i</sup>	DBT/Phen <sup>k,l</sup>	MPI-1 <sup>m</sup>	R <sub>C</sub> <sup>m</sup>					
Murta	J2/05	18.03	11.40	70.58	0.43	0.34	0.34	0.06	0.40	0.64					
	J2/06	20.37	10.90	68.73	0.31	0.29	0.29	0.24	0.43	0.66					
	W1/11	21.29	18.46	60.25	0.32	0.36	0.36	0.39	0.37	0.62					
	W1/17	19.03	13.59	67.39	0.44	0.38	0.38	0.32	0.39	0.63					
	T1/24	15.37	14.14	70.49	0.46	0.30	0.30	0.54	0.35	0.61					
	T1/26	20.17	12.63	67.20	0.40	0.34	0.34	0.35	0.35	0.61					
	T1/29	14.47	10.15	75.39	0.25	0.32	0.32	0.35	0.34	0.60					
	L8/42	18.39	16.58	65.03	0.27	0.20	0.20	0.27	0.28	0.57					
	L8/44	25.98	10.46	63.55	0.35	0.27	0.27	0.22	0.30	0.58					
	L7/45	15.55	14.07	70.38	0.37	0.24	0.24	0.26	0.31	0.59					
L7/46	23.44	14.00	62.55	0.37	0.37	0.37	0.19	0.30	0.58						

**Table 3** (continued)

Formation	Sample ID	GC–MS molecular fractions, ratios and indices						
		Steranes			Aromatics			
		$C_{27}$ (%) <sup>a,i</sup>	$C_{28}$ (%) <sup>a,i</sup>	$C_{29}$ (%) <sup>a,i</sup>	$C_{29} \alpha\beta/\alpha\beta\beta + \alpha\alpha\alpha^d$	$C_{29} \alpha\alpha\alpha / 20S/20S + 20R^j$	MPI-1 <sup>m</sup>	$R_C^m$
Birkhead	B5/34	22.17	12.24	65.59	0.49	0.44	0.38	0.60
	B5/35	13.99	13.50	72.50	0.47	0.43	0.37	0.61
	M4/37	15.02	12.21	72.77	0.44	0.43	0.51	0.49
	M4/40	12.47	10.48	77.05	0.42	0.42	0.48	0.49
	P1/55	11.51	15.63	72.86	0.44	0.43	0.65	0.54
	P1/56	9.70	12.08	78.21	0.43	0.45	0.63	0.54

Source-related biomarker ratios are in *italic*, all remaining parameters are maturity-related

<sup>a</sup>Peters et al. (2005a)

<sup>b</sup>Connan and Cassou (1980)

<sup>c</sup>Peters et al. (1999)

<sup>d</sup>Peters et al. (2005b)

<sup>e</sup>Scalan and Smith (1970)

<sup>f</sup>ten Haven and Rullkötter (1988)

<sup>g</sup>Fan et al. (1987)

<sup>h</sup>Seifert and Moldowan (1980)

<sup>i</sup>Moldowan et al. (1985)

<sup>j</sup>Seifert et al. (1981), Seifert and Moldowan (1986)

<sup>k</sup>Hughes et al. (1995)

<sup>l</sup>Masslen et al. (2011)

<sup>m</sup>Radke et al. (1982)

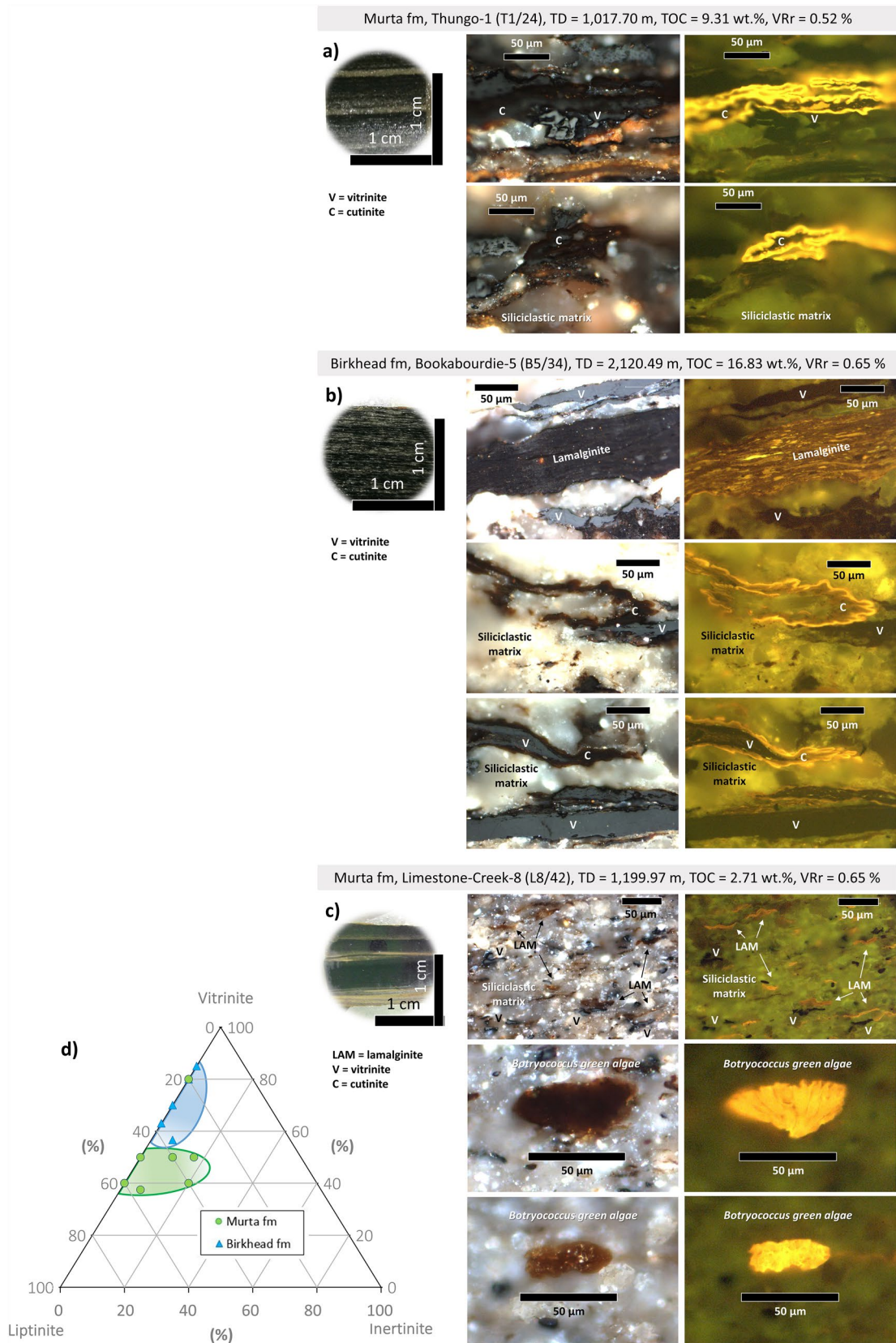




**Fig. 4** Microscopic details of dispersed organic matter (DOM) from petrographic maceral analysis (*left column*: reflected light; *right column* with fluorescence). **a** DOM in a representative sample of the Murta Formation (Thungo-1, sample T1/24): “cutinite flames” (bright yellow under UV-light) and vitrinite in the coarse siliciclastic matrix. **b** DOM in a representative sample of the Birkhead Formation (Bookabourdie-5, sample B5/34): thick lamalginite (yellow/brown), “cutinite flames” (yellow/orange) and vitrinite in coarse siliciclastic matrix. **c** DOM in the Murta Formation (Limestone-Creek-8, sample L8/42): abundant particles of fine lamalginite (orange/brown), vitrinite, and fragments and aggregates of *Botryococcus braunii* sp. (dark yellow) in a fine siliciclastic matrix. **d** Maceral composition of selected samples displayed in a ternary diagram (siliciclastic matrix subtracted): both formations contain little to no inertinite. The vitrinite content is generally higher in the Birkhead Formation, while liptinite (including cutinite, lamalginite, telalginite) dominates in the Murta Formation

### Normal and acyclic isoprenoid alkanes

Figure 5a shows the distribution of *n*-alkanes and isoprenoid alkanes in selected samples from the Murta and Birkhead formations. Whereas short-chain *n*-alkanes (*n*-C<sub>16</sub> to *n*-C<sub>20</sub>) are dominant in the Murta Formation, the Birkhead Formation features a more heterogeneous distribution of *n*-alkanes with additional distinct maxima in the long-chain range (*n*-C<sub>25</sub> to *n*-C<sub>27</sub>).

Pristane to phytane ratios (Pr/Ph) are moderate to high (Murta, 1.9–6.7; Birkhead, 4.6–9.9). Along with its higher Pr/Ph values, the Birkhead Formation also has higher pristane/*n*-heptadecane and phytane/*n*-octadecane values (see Table 3).

The *n*-C<sub>17</sub>/*n*-C<sub>27</sub> and terrigenous to aquatic ratios [TAR = (*n*-C<sub>27</sub> + *n*-C<sub>29</sub> + *n*-C<sub>31</sub>)/(*n*-C<sub>15</sub> + *n*-C<sub>17</sub> + *n*-C<sub>19</sub>)] show very similar diverging trends. The *n*-C<sub>17</sub>/*n*-C<sub>27</sub> ratio ranges from 0.31 to 1.41 in the Birkhead Formation (except sample M4/37) and from 2.1 to 65 in the Murta Formation (except sample T1/24). TARs of the Birkhead Formation range from 0.2 to 1.9, while in the Murta Formation they are less than or equal to 0.3. Sample T1/24 represents a special sample with TAR = 0.00 and *n*-C<sub>17</sub>/*n*-C<sub>27</sub> = 581 which may be representative of a lake facies with specific geochemistry and petrography. Odd-to-even predominance (OEP; after Scalán and Smith 1970; calculated according to Peters et al. 2005b) is very similar in both formations and varies between 1.0 and 1.2 (Murta Formation avg.: 1.07; Birkhead Formation avg.: 1.06). A correlation between TAR and Pr/Ph (as proposed by Hackley et al. 2020) was not observed.

### Alicyclic isoprenoids

Hopanes and steranes were detected in all samples in high concentrations permitting peak area calculation without strong background interference. Representative hopane (*m/z* 191) and sterane (*m/z* 217) distributions are shown in Fig. 5a.

The C<sub>19</sub>/C<sub>23</sub> tricyclic terpane ratio ranges between 2 and 13 in the Murta Formation and from 3 to 17 in the Birkhead Formation. The C<sub>29</sub>/C<sub>30</sub> hopane ratios of both formations fall in the same range between 0.50 and 0.69 (except sample T1/26 with a ratio of 1.03; Murta Formation avg.: 0.67; Birkhead Formation avg.: 0.59). Likewise, the terpane ratios  $T_S/(T_S + T_M)$ ,  $C_{29}T_S/(C_{29}T_S + C_{29}H)$  and  $C_{31}22S/(22S + 22R)$  (Table 3) indicate very similar maturities for both formations. However, the moretane to hopane ratio (C<sub>30</sub>M/(C<sub>30</sub> + C<sub>30</sub>M)) is generally lower in the Birkhead Formation (avg.: 0.14) than in the Murta Formation (avg.: 0.22).

The regular sterane distributions of both formations are dominated by the C<sub>29</sub> homologue, ethylcholestane (Table 3). Its maturity-dependent isomer ratios [ $\alpha\alpha\alpha$  20S/(20S + 20R) and  $\alpha\beta\beta/(\alpha\beta\beta + \alpha\alpha\alpha)$ ] show a broader scatter for the Murta Formation (0.20–0.38; and 0.25–0.46) and a narrow range at generally higher values for the Birkhead Formation (0.42–0.45; 0.43; and 0.42–0.49). The salinity indicator gammacerane and the angiosperm biomarker oleanane (Moldowan et al. 1994) were not identified.

### Aromatic compounds

Quantification of phenanthrene (Phen) and its methyl homologues, i.e. 3-, 2-, 9-, and 1-methylphenanthrene as well as dibenzothiophene (DBT, after Hughes et al. 1995; Maslen et al. 2011) resulted in DBT/Phen ratios ranging from 0.06 to 0.54 in the Murta Formation and from 0.31 to 0.65 in the Birkhead Formation (compare Fig. 5b).

Values of the Methylphenanthrene Index (MPI-1, after Radke et al. 1982) range between 0.14 and 0.35 for the Birkhead Formation, and from 0.28 to 0.43 in the Murta Formation resulting in calculated vitrinite reflectances ( $R_C$ , after Radke et al. 1982) of 0.49 and 0.61% for the Birkhead Formation and 0.57–0.66% for the Murta Formation.

### Discussion

Evaluation of the new geochemical and petrographic data presented in Tables 2 and 3 has involved rigorous comparison with existing data sets and interpretation based on established classification schemes. The values of a given parameter should be regarded with caution since biochemical and thermal processes may counteract each other. Thus, only the combination of multiple parameters allows for reliable conclusions.

The two fluvio-lacustrine formations and the analysed core sections are not continuous. Therefore, the observed heterogeneity of the two potential source rocks and the limited core data do not allow the determination of representative net/gross ratios. Even the combined core length at a single well location (see Table 10) is rarely representative

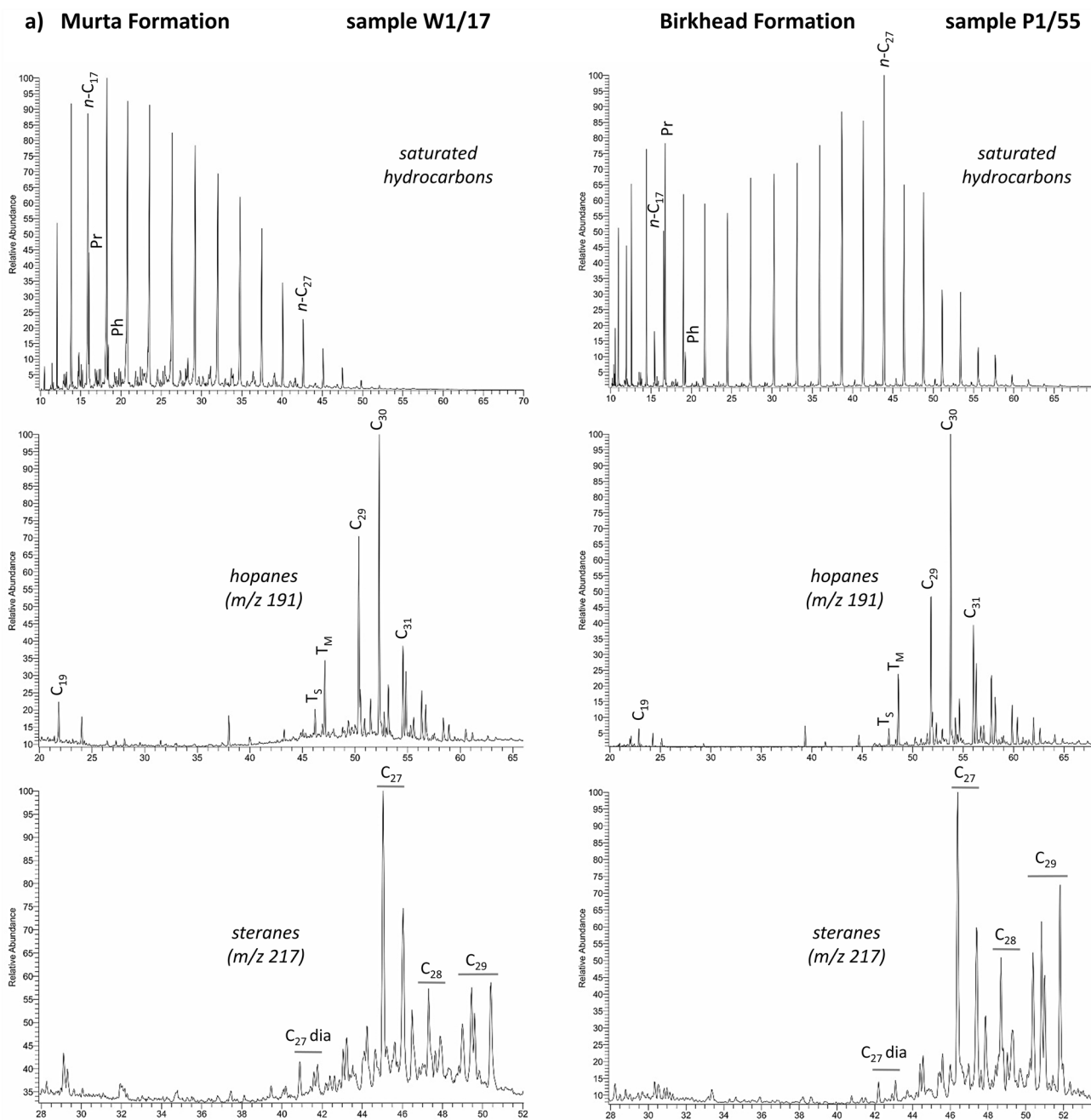


**Fig. 5** GC-FID/GC–MS chromatograms with signal intensities of molecular compounds from representative samples of both analyzed formations. **A** Saturated hydrocarbons, hopanes and steranes (*left* Murta Formation, sample W1/17; *right* Birkhead Formation, sample P1/55). **B** Aromatic hydrocarbons, tri-methylnaphthalenes (TMNs) and tetra-methylnaphthalenes (TeMNs) (*left* Murta Formation, sam-

ple W1/17; *right* Birkhead Formation, sample P1/55). *Stippled lines* (slopes between the peaks) are explained in the discussion chapter under ‘thermal maturity’. Only the most important biomarkers are labelled (abbreviations/peak IDs explained in supplementary information table S3)

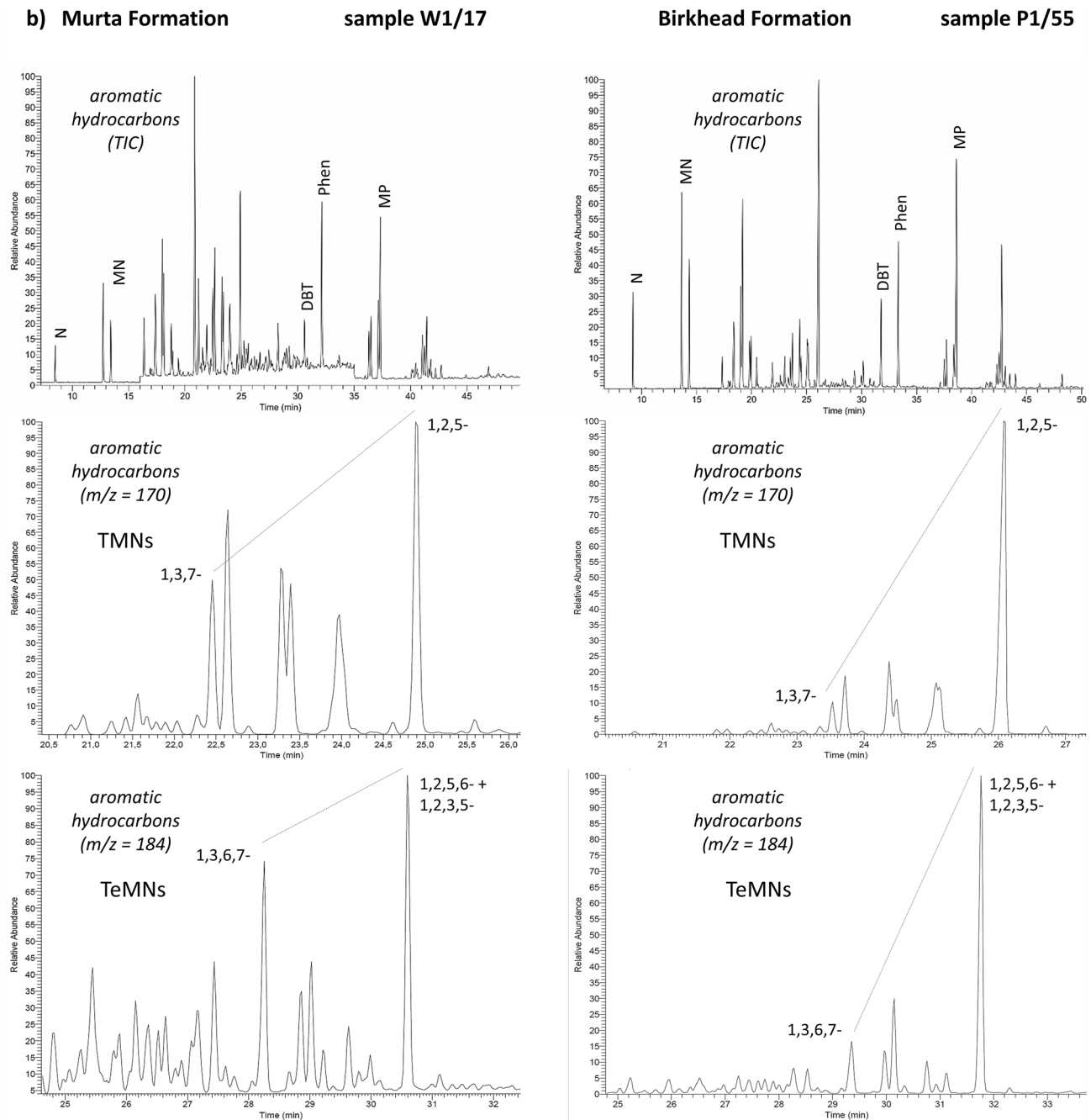


Fig. 5 (continued)

of the entire formation thickness. According to the regional 3D model of Hall and Palu (2016), the respective maximum thickness of the Birkhead and Murta formations are 150 & 80 m. Furthermore, their present sampling was conducted with a focus on fine-grained, organic-rich lithofacies- and not at a regular interval. Therefore no true geochemical logs can be provided. In the following sections, we systematically discuss our results in the context of paleo-depositional environment, thermal maturity and source rock potential. In

Table 4, we summarize the main source rock properties of the Birkhead and Murta formations.

### Biological precursors and paleo-depositional environment

The carbon and sulphur cycles are strongly interrelated in sedimentary systems. According to Berner (1984) and Berner and Raiswell (1984), a generally positive relationship

between TOC and  $T_S$  exists in environments with oxygenated bottom waters, but not in anoxic settings. Further, sediment sulphur contents are much higher in marine and brackish water environments. Sulphur is present both as iron sulphides (pyrite & marcasite) and organic compounds formed during early diagenesis (Sawlowicz 1993), declining with decreasing availability of dissolved sulphate. Therefore,  $T_S/TOC$  ratios are usually much higher in marine water than in sulphate-depleted freshwater. Thus, modern “normal”, non-anoxic, marine sediments have TOC/ $T_S$  ratios close to 2.8:1. The TOC/ $T_S$  values of both formations scatter around 80:1 (Fig. 6a), indicative of freshwater conditions and supporting the presence of sulphate-depleted waters during their deposition. They provide no evidence of the previously reported brackish conditions in the Murta Formation.

The maximum TIC value of 3.3% (T1/27) converts to 27.7% CaCO<sub>3</sub> and corresponds with the minimum TOC and  $T_S$  values (TOC = 0.5%,  $T_S$  = 0.05%). Under the microscope, amorphous crystalline material is visible, which occupies most of the intergranular space between the silt and fine sand grains (about 60 µm diameter) and which can be characterized as phreatic carbonate cement. This exceptional interval therefore either represents an eogenetic calcrete horizon due to temporarily high evaporation rates during deposition of the lower (more shallow and more fluvial) successions of the Murta Formation (Unit 1 or 2, see Sect. 2.2), or it was caused by mesogenetic calcite cementation (compare e.g. Schulz-Rojahn 1993). The otherwise very low TIC values in all other samples are as expected for deposition in fresh water.

Langford and Blanc-Valleron (1990) developed a diagram to classify the three main kerogen types (type I = algal/lacustrine; type II = planktonic/marine; and type III = land plant/terrigenous) based on the relationship between  $S_2$  and TOC. In the “Langford plot” (Fig. 6b) the Murta Formation samples scatter around the boundary between type II and type

III kerogen with a preference towards type III, while the Birkhead samples predominantly yield type II kerogen.

As displayed in the classification scheme after Espitalié et al. (1985), kerogen types can also be determined based on the relationship between HI and Rock–Eval  $T_{max}$  (Fig. 6c). While the range of measured  $T_{max}$  is very similar for both formations (all samples plot around the onset of the indicated oil window), the HI of the Birkhead Formation is generally higher than that of the Murta Formation. The maximum and minimum HI values were obtained from the Poonarunna-1 (Birkhead) and Jackson-2 (Murta) samples, respectively. Here—as in the “Langford plot” (Fig. 6b)—the Birkhead Formation is shown to contain type II kerogen, and the Murta Formation type II/III kerogen. This appears contrary to the *n*-alkane distributions of the Birkhead Formation which reflect a heterogeneous mix of algal, bacterial and land-plant hydrocarbons, while those of the Murta Formation are unimodal and less enriched in the waxy C<sub>23+</sub> homologues (Fig. 5a).

As pointed out by Connan and Cassou (1980), the Pr/*n*-C<sub>17</sub> and Ph/*n*-C<sub>18</sub> ratios help to distinguish kerogen types and depositional environments. In a log/log diagram (modified after Peters et al. 1999 with customized axis minima) the Murta Formation plots with some unusually low values at the boundary between type III and mixed type II/III kerogen (Fig. 6d). With predominantly Pr/*n*-C<sub>17</sub> > 1, the Birkhead Formation data indicate type III kerogen and deposition under oxidizing, swampy conditions (Lijmbach 1975). This interpretation is not affected by biodegradation (Peters et al 2005b), i.e. abundant *n*-alkanes and the absence of a distinct hump in the chromatograms related to unresolved complex mixture (UCM) indicate that no significant biodegradation occurred (Hedges et al. 2000; Fig. 5a) as expected for fine-grained rocks.

With TAR = 0.0 and *n*-C<sub>17</sub>/*n*-C<sub>27</sub> = 581, Murta sample T1/24 represents a quiet, purely aquatic environment. Indeed, macroscopically recognizable and undisturbed

**Table 4** Summary of the main source rock characteristics of the Murta and Birkhead formations

Parameter/formation	Birkhead	Murta
Depositional environment	Meandering fluvial, floodplain	Fluvio-lacustrine
Total organic carbon content (TOC)	1.0–16.8 (average: 3.7) wt. %	0.5–9.3 (avg.: 2.2) wt. %
Vitrinite reflectance (VR <sub>r</sub> )	0.54–65% (early oil window)	0.52–73% (early oil window)
Rock–Eval $T_{max}$	427–439 °C	425–440 °C
Relative maceral group content	Vitrinite > liptinite > inertinite	Liptinite > vitrinite > inertinite
Pristane/Phytane ratio (Pr/Ph)	4.55–9.92 (terrigenous)	1.93–6.74 (oxic/terrigenous)
Typical saturate chromatogram maxima	<i>n</i> -C <sub>15</sub> to <i>n</i> -C <sub>17</sub> , and <i>n</i> -C <sub>25</sub> to <i>n</i> -C <sub>27</sub>	<i>n</i> -C <sub>16</sub> to <i>n</i> -C <sub>20</sub>
Hydrogen Index (HI)	184–436 (avg.: 300) mg HC/g TOC	28–268 (avg. 150) mg HC/g TOC
Kerogen types	Mixed type II/III, mixed type I/III	Mixed type II/III
Generation potential (GP)	Fair to very good	Poor to very good
Production index (PI)	0.03–0.18	0.05–0.65
Approximate onset of oil window	> 440 °C / > 0.7 VR <sub>r</sub> %	< 425 °C / < 0.45 VR <sub>r</sub> %

varvites (see Fig. 3) indicate deposition in a low-energy environment. The occurrence of fossil *Botryococcus* sp. (found as telalginite in sample L8/42; Fig. 4c) represents planktonic green algae colonies that live only in fresh to brackish water settings and are common in terrestrial/lacustrine petroleum source rocks (Moldowan and Seifert 1980; McKirdy et al. 1986a; Glikson et al. 1989; Metzger and Largeau 2005; Blumenberg et al. 2019). The input of such algae might augment the abundance of  $C_{27}$ – $C_{31}$  *n*-alkanes (Moldowan et al. 1985; Derenne et al. 1988) which are more commonly attributed to land-plant input.

The  $C_{19}/C_{23}$  tricyclic terpane ratio is also sensitive to differences in OM input (Peters et al. 2005a).  $C_{19}$  and  $C_{20}$  tricyclic diterpanes originate from higher land plants (e.g. Alberdi et al. 2001), whereas extended tricyclic terpanes ( $C_{21}$ +) derive from algae and bacteria (Ourisson et al. 1982; Moldowan et al. 1983; Zumberge 1987). Sources of OM can therefore be distinguished by low (marine < 1) and high (terrigenous > 1)  $C_{19}/C_{23}$  values. All the samples in Table 3 have  $C_{19}/C_{23}$  tricyclic ratios > > 1, consistent with the predominantly land plant origin of their OM.

The  $C_{29}/C_{30}$  hopane ratio serves as a lithological indicator, discriminating between carbonate and argillaceous rocks and their derived crude oils (Fan et al. 1987; ten Haven & Rulkotter, 1988; Peters et al. 2005b). Except for Murta sample T1/26, all samples in Table 3 have values < 0.75, consistent with their siliciclastic character.

The ternary diagram of Huang and Meinschein (1979) shows a clear dominance of  $C_{29}$  steranes indicating a major input of OM from higher land plants. This signal is particularly strong in the Birkhead Formation.

Hughes et al. (1995) introduced the zonation of depositional environments based on the relationship between Pr/Ph and DBT/Phen ratios. The DBT/Phen ratio helps discriminate between carbonate- and clay-rich lithofacies (Hughes et al. 1995; Maslen et al. 2011). According to this classification, all samples belong to the clay-rich series (Fig. 6f). While the Murta Formation formed under oxic fluvio-lacustrine conditions (Zones 3/4), the Birkhead Formation incorporates more highly oxidised terrigenous OM that accumulated in an oxic fluvio-deltaic/swampy milieu (Zone 4). With only one exception (Murta T1/26), the two formations can be clearly distinguished as containing two different mixes of OM. The highest Pr/Ph ratios occur at Moorari-4 (6.7, 9.9), followed by samples from Poona-runna-1 (6.0, 6.4) and Bookabourdie-5 (4.5, 5.2), respectively. With high but variable input from land plants, all Birkhead Formation samples are therefore attributable to the terrigenous (fluvial/deltaic) zone. Murta samples from Thungo-1 display the highest Pr/Ph ratios (3.4, 3.6 and 6.7), followed by those from Limestone Creek-7 (3.1 and 3.3), all consistent with fluvial/deltaic conditions. The remaining Murta samples have values between 2 and 3, reflecting more

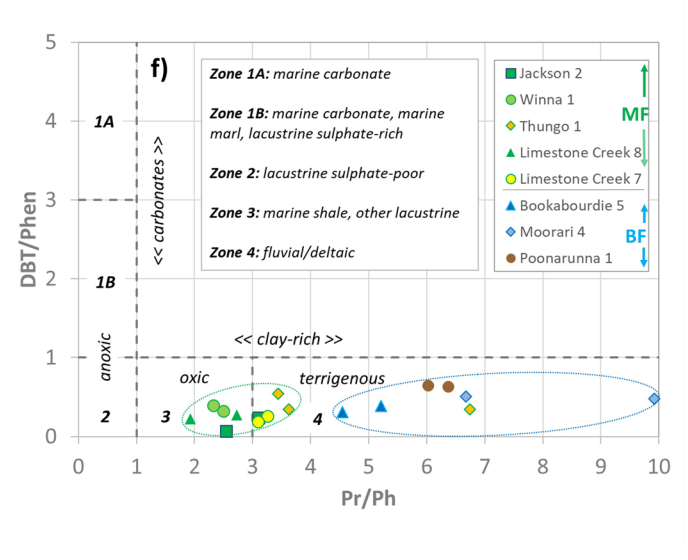
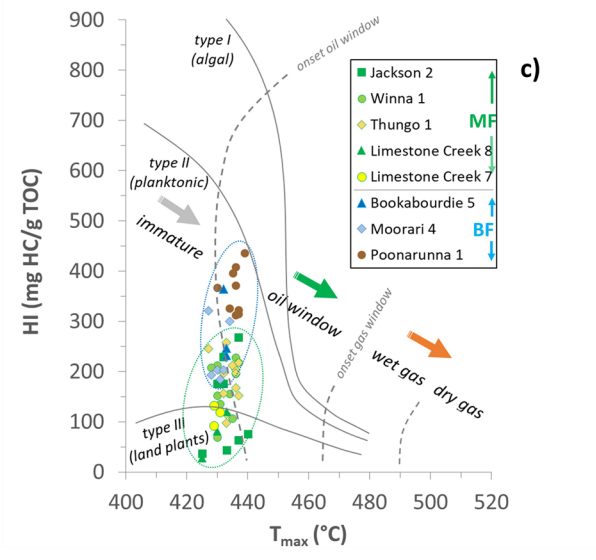
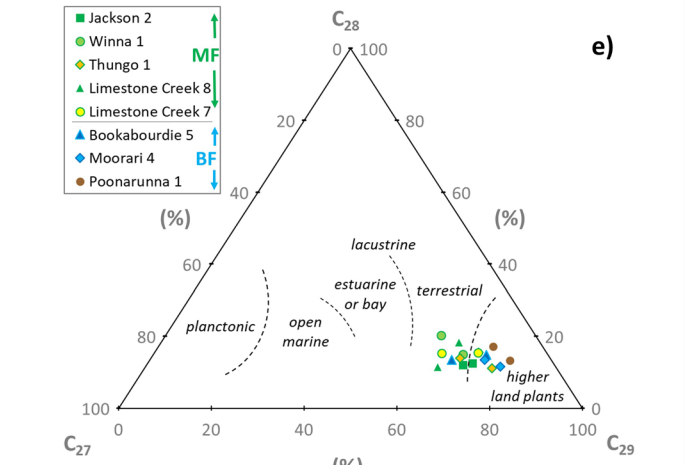
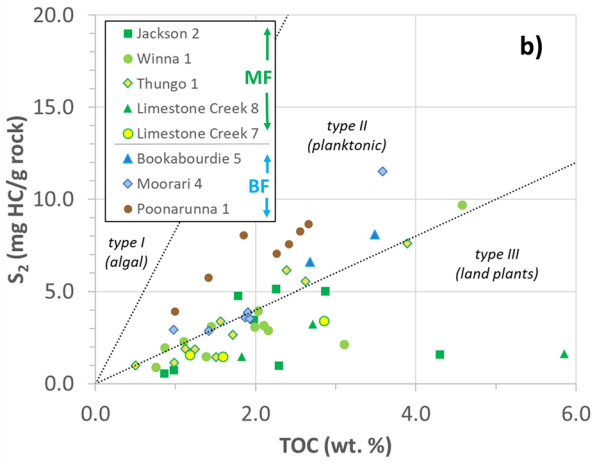
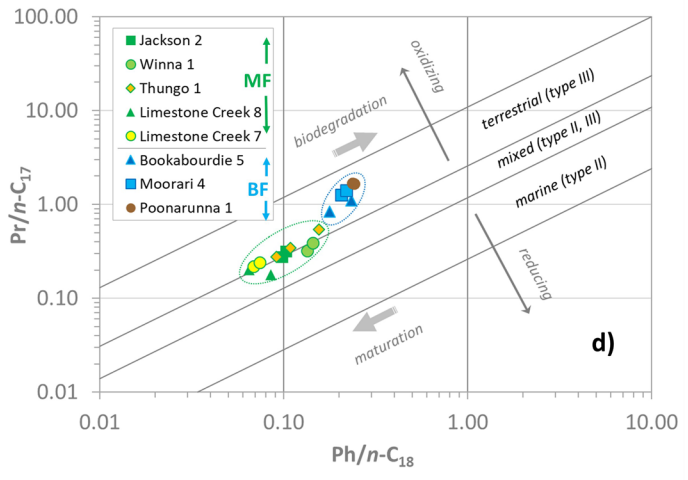
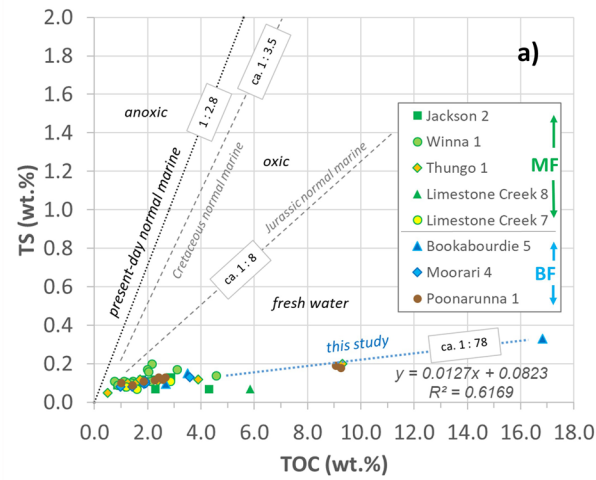
distal lacustrine depositional environments. The absence of gammacerane (a typical salinity indicator after Sinninghe Damsté et al. 1995) in all samples also indicates fresh-water conditions.

Relative distribution of macerals (Fig. 4d) and corresponding HI values (Table 2, Fig. 6c) indicate bacterially enriched terrigenous OM present in the Murta Formation. Earlier studies found evidence of mixed algal OM with terrestrial organic detritus that accumulated in a fresh-water to the brackish lacustrine environment (Ambrose et al. 1986; Michaelsen and McKirdy 1989). While this is in principal agreement with our results, we see little evidence of brackish conditions (see very low S/TOC ratios).

Dominance of vitrinite in the Birkhead Formation (Fig. 4d) clearly indicates terrigenous kerogen (type III). The rather high HI values are consistent with earlier observations (e.g. Khorasani 1987) and are related to terrigenous organic facies containing abundant hydrogen-rich liptinite, mainly represented by cutinite and sporinite (e.g. Jenkins 1989; Hawkins et al. 1989). Additionally, microbial decay of vitrinite could have added biomass of archaea and other bacteria modifying HI values (Table 2; Fig. 6c) of the Birkhead Formation (Powell 1986; Boreham and Summons 1999). The undisturbed laminations observed on the core (Fig. 3) indicate a relative quiet water body and a lesser degree of bioturbation during deposition of the Birkhead Formation.

Although we could not clearly assign our results to the individual Birkhead Formation units after Paton (1986), we can confirm a calm, oxic and purely terrestrial paleo-depositional environment for this formation. Our findings accord with the previously assigned meandering, high-sinuosity, deltaic to fluvio-lacustrine conditions (e.g. Veevers 1984; McIntyre et al. 1989; Lanzilli, 1999) that characterized the “Lake Birkhead” floodplain (Mackie and Gumley 1995; Boulton et al. 1997). However, the brackish paleo-depositional conditions inferred by Burger (1986) are not confirmed by our study. Due to the observed cross-bedding and coarse detritus (Fig. 3), the investigated samples belong to the fluvial successions (Unit 1 and Unit 3 after Paton 1986) rather than to the swampy/lacustrine interval (Unit 2; compare Sect. 2.1).

Featuring a relatively dynamic and predominantly oxic fluvio-lacustrine paleo-depositional environment with sporadic blooms of fresh-water *Botryococcus* green algae, the Murta Formation represents the Australian example of common Early Cretaceous fluvio-lacustrine deposits such as the English Purbeckian and German Wealden facies (Blumenberg et al. 2019). Since we found no evidence for deep-water/offshore sedimentation and marine transgression (compare Veevers et al. 1991), we assign the investigated Murta Formation samples to the lower successions of the Murta Formation (Units 1 and 2 after Ambrose et al. 1982, 1986; see also Sect. 2.2), which mainly represent shallow



water and fluvio-lacustrine/deltaic conditions. Similarly, fluvio-lacustrine paleo-depositional conditions of the proposed “Lake Murta” (Gorter 1994; Alexander et al. 2006) were confirmed by our study.

**Thermal maturity**

In Fig. 7a, both formations cluster between 0.5 and 0.7 VR<sub>t</sub> and 425 to 440 °C T<sub>max</sub>. Given their vitrinite-rich maceral assemblages (Fig. 4d), vitrinite reflectance is a reliable

**Fig. 6** Elemental composition, source-related Rock–Eval parameters and source-related biomarkers. **a** The relation between total sulphur content (TS) and total organic carbon content (TOC) subdivided into Murta Formation (*green circles*) and Birkhead Formation samples (*blue triangles*). Classes of the depositional environment (anoxic, oxic, fresh water), present-day normal marine line, as well as Cretaceous and Jurassic normal marine paleo-lines (after Berner 1984 and Berner and Raiswell 1984). **b** Simple differentiation of kerogen type (source of organic matter) based on Rock–Eval S2 vs. TOC displayed as “Langford-plot” (classification after Langford and Blanc-Valleron 1990) and separated by individual wells (excluded samples/outside diagram: T1/24, B5/34, P1/55, P1/56). **c** Hydrogen Index (HI) vs Rock–Eval  $T_{max}$  with kerogen type classification and onset of oil/gas windows after Espitalié et al (1985). *Green ellipse*=Murta fm, *blue ellipse*=Birkhead fm. **d** Logarithmic cross plot of pristane/ $n$ -C<sub>17</sub> and phytane/ $n$ -C<sub>18</sub> ratios showing the depositional milieu and origin of organic matter of the analyzed samples (after Connan and Cassou 1980, modified after Peters et al. 1999). **e** Ternary diagram with relative content of sterane compounds C<sub>27</sub>, C<sub>28</sub>, C<sub>28</sub> for classification of organic matter origin (after Huang and Meinschein 1979). Both formations yield terrestrial paleo-depositional milieu. **f** Cross-plot of DBT/phenanthrene vs pristane/phytane for the classification of the depositional environment (zonation after Hughes et al. 1995). The Murta Formation indicates lacustrine to fluvial conditions, while the Birkhead Formation plots in the fluvial/deltaic zone

maturity parameter (Hartkopf-Fröder et al. 2015). Based on the typical onsets of the respective oil windows for type II and type III kerogen (after Tissot and Welte 1984), the samples range from immature to early mature for oil generation. However, only Birkhead Formation samples from Poonarunna-1 are located inside the early oil window. All the other Birkhead Formation samples are immature. There is some moderate scatter within individual boreholes, which can be expected. “Suppression” of vitrinite reflectance is unlikely because both formations contain abundant non-fluorescing vitrinite. As compared to coals, in such environments vitrinite reflectance shows more scatter, but the same average values and depth trends (Scheidt and Littke 1989).

The HI is an indirect maturity indicator, helping to distinguish kerogen types and their respective maturation pathways (Espitalié et al. 1985; Law 1999). Figure 6c demonstrates the relationship between HI and  $T_{max}$  and shows a different field for each formation. The Murta samples have relatively low HI values and contain thermally immature kerogen ranging in composition from type II/III to type III. The Birkhead samples have generally higher HI values characteristic of type II to type II/III kerogen, those from Poonarunna-1 being located within the early oil window for type II kerogen (VR > 0.5%).

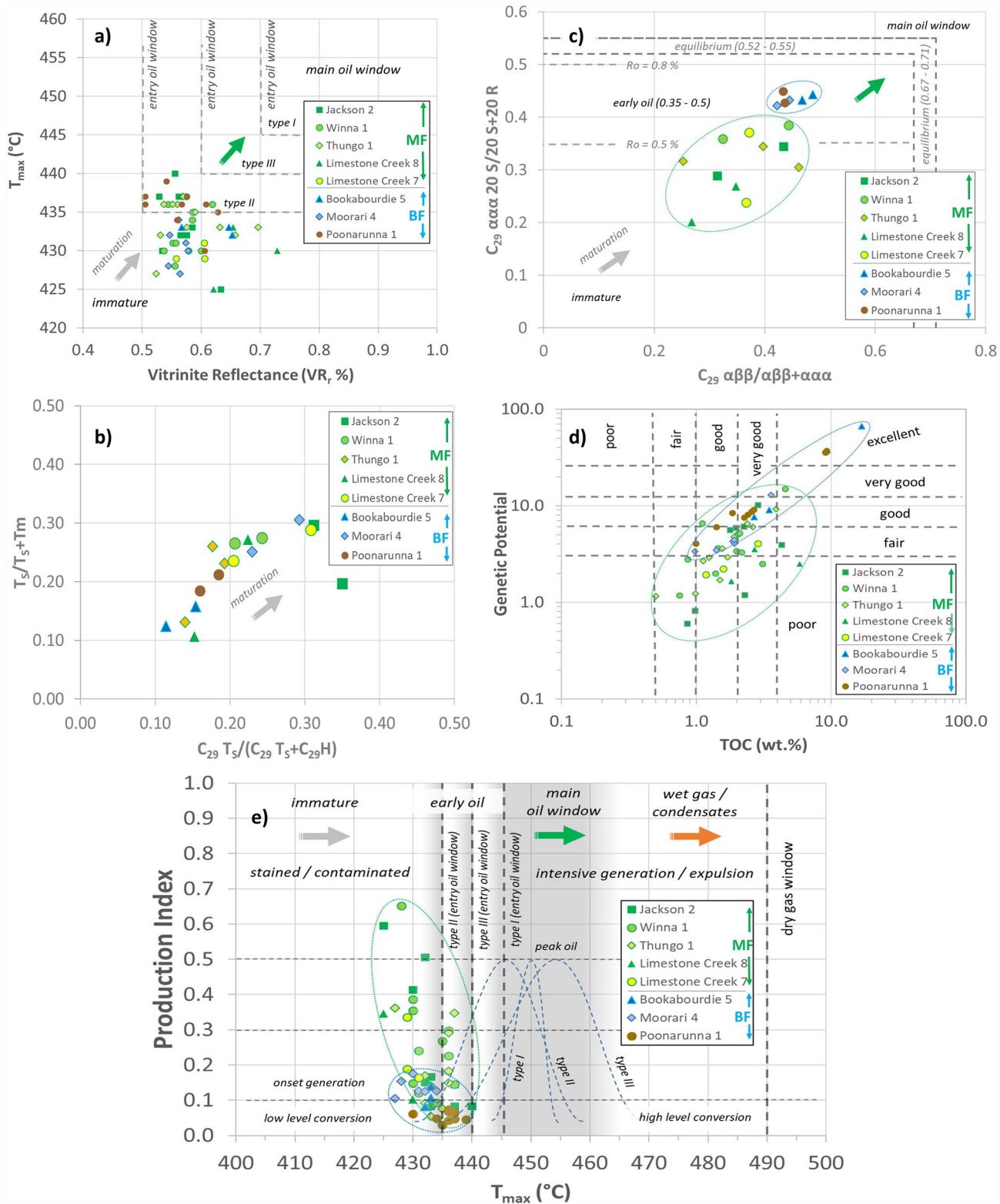
Maturity-related biomarker ratios of the subsamples deliver partly contradicting interpretations. Values between 1.0 and 1.2 for the odd-to-even predominance (OEP) of  $n$ -alkanes are surprisingly low in all samples, with those from Poonarunna-1 (Birkhead Formation) and Winna-1 (Murta Formation) being the closest to 1 and indicating the highest maturity.

Terpane ratios  $T_s/(T_s + T_m)$  and  $C_{29}T_s/(C_{29}T_s + C_{29}H)$  typically increase with maturity (Peters et al. 2005a), in this case indicating that of its three sample locations the Birkhead Formation is most mature at Moorari-4 and least mature at Bookabourdie-5. No clear trend in these parameters is evident for the Murta Formation (Fig. 7b). Conversely, the moretane to hopane ratio  $C_{30}M/(C_{30}M + C_{30}H)$  decreases with increasing maturity, from 0.8 to 0.05 (Seifert and Moldowan 1980). This parameter suggests that the Birkhead Formation is more mature than the Murta Formation, contrary to the vitrinite reflectance and Rock–Eval data. Thermal maturation also causes a stereochemical rearrangement of the C<sub>31</sub> homohopane epimers towards an endpoint 22S/(22S + 22R) ratio of 0.58–0.62 (Seifert and Moldowan 1980). The Birkhead values lie within this range, while those of the Murta Formation are somewhat lower with only three exceeding 0.58.

$C_{29}$   $aaa$  20S/(20S + 20R) and  $C_{29}$   $\alpha\beta\beta$ /( $\alpha\beta\beta$  +  $aaa$ ) are sterane parameters commonly used to evaluate immature to early mature rock samples. Their equilibrium values are 0.55 and 0.71, respectively, roughly equivalent to the transition from the early to the main oil window ( $R_o$  ~ 0.8–0.9%; Seifert and Moldowan 1986; Peters et al. 2005a). As displayed in Fig. 7c, the Birkhead Formation plots in a small area entirely within the early oil window, while the Murta Formation shows a broader scattering at the transition from immature to early mature. Biomarker-based thermal maturity seems to be generally slightly higher and more homogeneous in the Birkhead Formation than in the Murta Formation.

The Methylphenanthrene Index (MPI-1, after Radke et al. 1982) correlates with thermal maturity and allows the calculation of equivalent vitrinite reflectance ( $R_C$ ). The obtained  $R_C$  values of the Murta Formation fall between 0.58 and 0.66% with local variations providing higher values for the Jackson-Naccowlah-Pepita Ridge compared to the Murteree Ridge, with those from Jackson-2 being the highest. Oil staining of individual samples from Jackson-2 and Winna-1 proves petroleum generation and expulsion at these sites. Thus, a variable but mostly low thermal maturity at the onset of oil generation is confirmed. Subtle differences should not be over-interpreted, since this parameter is better suited to higher maturities (Radke et al. 1982).

Multiple maturity-related parameters are in accordance with a narrow zone around the transition from immature to the early oil window. Poonarunna-1 seems to represent the high maturity end-member with all samples occupying the early oil window. Several parameters indicate a slightly higher thermal maturity for Birkhead Formation than for Murta Formation (Fig. 6c, 7a, c, and e), but not Pr/ $n$ -C<sub>17</sub> and Ph/ $n$ -C<sub>18</sub>, which show the opposite trend. The distributions of trimethylnaphthalenes (TMNs) and tetramethylnaphthalenes (TeMNs) (Fig. 5b) indicate a low



maturity for each formation (compare van Aarssen et al. 1999), although the Murta displays a higher relative abundance of the stable isomers.

The majority of the samples in Table 2 have a low thermal maturity (immature to early oil window, ~0.55% VR<sub>r</sub>) making it likely that the measured TOC and HI values are not much different from their original values prior to



**Fig. 7** Maturity-related Rock–Eval parameters, maturity-related biomarkers and hydrocarbon potential. **a** Thermal maturity expressed as the relation between Rock–Eval  $T_{\max}$  vs. vitrinite reflectance. Onset of kerogen-dependent oil window after Tissot and Welte (1984). **b** Terpanes maturity-related ratios  $T_s/T_s + T_m$  vs.  $C_{29}T_s/C_{29}T_s + C_{29}H$  (after Peters et al. 2005a, b). Both formations show relative low thermal maturity. **c** Cross-plot of isomerization ratios for  $C_{29}$  20S/20 s + 20R vs.  $C_{29}$   $\beta\beta/\beta\beta + \alpha\alpha$  steranes (equilibrium values (dashed lines after Seifert and Moldowan 1980, 1986). **d** Source rock potential according to the logarithmic illustration of the genetic potential ( $GP = S_1 + S_2$ ) vs. TOC based on the classification after Hunt (1996) and Peters and Cassa (1994). **e** Produced hydrocarbons based on Production Index (PI) vs. Rock–Eval  $T_{\max}$ . Boundaries of conversion (onset generation,  $PI = 0.1$ ; peak oil,  $PI = 0.5$ ) after Law (1999); onset of kerogen-dependent oil window after Tissot and Welte (1984), shapes of kerogen-dependent generation curves are approximated and not data-based

burial. Our results confirm that the Birkhead Formation does not generate substantial amounts of hydrocarbons below 0.55% VRr. Accordingly, oil expulsion is expected to have been very limited (Deighton et al. 2003). The sample locations of the Murta Formation are situated along two ridges bounded by deep-seated inverted faults—the Jackson–Naccowlah–Pepita and the Murteree ridges, which represent important tectonic features of the stacked basin system (Apak et al. 1997). Episodes of sedimentation and post-sedimentary uplift and erosion caused multiple unconformities in the study area (e.g. Winton Unconformity) and could therefore influence thermal maturity. While volcanic/magmatic influence near the sampled wells is unlikely, hydrothermal circulation along deep faults could also provide focussed alterations of the temperature field. In future studies, detailed thermal modelling could help to constrain the thermo-tectonic evolution of the Eromanga Basin and the underlying Cooper Basin.

### Petroleum generation potential

To identify the origin of hydrocarbons in source rock samples the Oil Saturation Index ( $OSI = S_1 \times 100/TOC$ ) was introduced by Jarvie (2012). An OSI value of 100 serves as the boundary between rock samples containing indigenous and/or nonindigenous hydrocarbons. During programmed pyrolysis, most samples yielded indigenous hydrocarbons, but the exceptional OSI values of several samples from Jackson-2 (J2/06 and J2/07), Winna-1 (W1/17) and Thungo-1 (T1/24) (Table 2) indicate staining by oil expelled from deeper source rocks, or generation and expulsion from elsewhere within the formation.

Unusually high  $n-C_{17}/n-C_{27}$  ratios and terrestrial/aquatic ratios (TARs) close to zero in many Murta Formation samples could be an additional indicator of non-expulsion or staining from nearby petroleum sources. Contamination from drilling mud seems unlikely since water-based products (South

Australia: NaCl polyacrylamide, Queensland: KCl polymer, according to well completion reports) were applied and clean core samples (no cuttings) were investigated. Interestingly, there is no clear correlation between  $n-C_{17}/n-C_{27}$  and PI (compare Tables 2, 4). Contamination from younger ‘marine’ formations (e.g. Toolebuc Formation) can also be excluded since oleanane as well as  $C_{30}$  desmethyl and methylsteranes (Boreham and Powell 1987) are absent in all samples.

The relationship between generation potential ( $GP = S_1 + S_2$ ) and TOC can be illustrated using the log/log-diagram of Peters and Cassa (1994) and Hunt (1996). This plot (Fig. 7d) reveals poor to very good GP for the Murta (1–36 mg HC/g rock) and fair to excellent GP for the Birkhead (3–67 mg HC/g rock; see Table 4). The correlation between GP and TOC is stronger for the latter formation. The moderate to high PI values of most Murta samples (mainly between 0.1 and 0.5) are unexpected and may be due to indigenous oil generated from early-mature lamalginite. This is in agreement with previous studies, which reported an early onset of oil generation at approximately 0.45 VR<sub>r</sub> % (e.g. Powell et al. 1989; Wecker 1989). In contrast, the minor occurrence of *Botryococcus* algae might not suffice for measurable oil generation. For such *Botryococcus* facies, kinetics studies (e.g. Ziegs et al. 2015) indicate late oil generation, which does not fit to the situation observed here. Further, given that the underlying Birkhead Formation is oil-mature in the area of the JNP Ridge (e.g. Vincent et al. 1985), generation and upward migration of Birkhead oil is possible (compare Figs. 1b, 2b).

The Birkhead samples from Bookabourdie-5 and Moorari-4 show initial generation, but their PI remains below 0.2 (Fig. 7c). Assuming the presence of similar kerogen near the JNP Ridge, slightly higher thermal maturity could cause expulsion and migration of Birkhead oil into overlying strata including the Murta Formation. To detect and quantify oil mixing a separate study of locally reservoirized oils is required, such as those undertaken by Boreham and Summons (1999), Michaelsen and McKirdy (2001) and Arouri et al. (2004). However, as long as the source for contamination remains uncertain, even lateral self-charging of the Murta Formation cannot be ruled out.

Based on its maceral composition, a better oil generation potential can be expected for the liptinite-rich Murta Formation as compared to the vitrinite-rich Birkhead Formation (Table 4). However, Rock–Eval HI values tend to be higher in the Birkhead Formation (Fig. 6), although there is some overlap between the two units. This discrepancy may be related to the lower TOC values in the Murta and thus mineral-matrix effects during Rock–Eval pyrolysis (Peters 1986; Michaelsen 2002), but more probably to i) differences in thermal maturity, and ii) the presence of submicroscopic liptinite and per-hydrous vitrinite in the Birkhead Formation, which could not be petrographically identified.

Interestingly, all the Birkhead samples from Poona-runna-1 show very low conversion levels ( $PI < 0.1$ ), although the respective oil window for type II kerogen (Tissot and Welte 1984) has been already entered (compare Fig. 7a, c). However, Poona-runna-1 is located well outside the Cooper depocentre (Fig. 1a) and may represent somewhat different organic facies. Indeed, the high HI values of the Poona-runna-1 samples might indicate the incorporation of type I kerogen, which is known for a relatively late onset of oil generation at approximately 0.7 VR<sub>r</sub> %. Exceptional HI values above 700 mg TOC/g rock in particular Birkhead Formation samples observed by Mahlstedt and Horsfield (2016) support this argument.

The average organic richness of the Birkhead Formation (3.7% TOC: Table 2) is higher than earlier reported (2.5% TOC: Jenkins 1989), but this could be due to the focus on organic-rich beds during sampling. Hydrogen indices from the Birkhead Formation (184–436 mg HC/g TOC, avg. = 305 mg HC/g TOC) generally fall into the previously established range (150 and 500 mg HC/g TOC; McKirdy et al. 1986b; Michaelsen 2002; Boreham and Summons 1999; Mahlstedt and Horsfield 2016).

The organic richness of the Murta Formation (0.5–9% TOC) turned out to be higher than previously reported (0.5–2.5% TOC: Michaelsen and McKirdy 1989; Draper 2002), while the corresponding HI values (range = 28–268, avg. 153) appear slightly lower than those recorded by other workers (80–553: Michaelsen and McKirdy 1989, 2006; Powell et al. 1991; Boreham and Summons 1999).

Based on the results of this study and in contrast to some earlier publications, we consider the Murta and Birkhead formations to be efficient moderate-quality source rocks of the Eromanga petroleum system, although located at relatively shallow depths. Their organic matter contents and petroleum generation potentials are generally sufficient for oil expulsion when thermal maturation has reached the early oil window. Lateral variations of thermal maturity are primarily related to differences in burial depth and amounts of Late Cretaceous erosion across the study area. Based on our modelling results (Röth and Littke 2022), localized Middle Cretaceous magmatism in the Nappamerri Trough also might have influenced the thermal maturity of these Jurassic and Cretaceous source rocks. Therefore, any oil that has migrated from them may be expected to have accumulated in overlying sandstone intervals along fault-bounded inversion structures and near intrusive bodies within the Eromanga Basin.

## Conclusions

New organic petrographic and organic geochemical data acquired on a suite of 55 core samples provide further information on the source rock potential and the biomarker

composition of the siliciclastic fluvio-lacustrine Murta and Birkhead formations. Both source rock intervals are members of the Early Jurassic to Early Cretaceous fluvio-lacustrine succession (194–130 Ma) within the central Eromanga Basin and share several petrographical and geochemical similarities, but also display some significant compositional differences.

The siltstones and fine sandstones of the Middle Jurassic Birkhead Formation and the Early Cretaceous Murta Formation formed in isolated intracontinental fresh-water lacustrine settings. Very low total sulphur and inorganic carbon contents, the absence of gammacerane, low dibenzothiophene/phenanthrene ratios and very high pristane/phytane ratios together clearly indicate oxic, non-marine conditions.

Both formations contain fair to excellent concentrations of organic matter which exhibits fair to very good hydrocarbon generation potential. Their type II and type II/III kerogens are derived mainly from higher land plants, with lesser contributions from green algae and bacteria. Vitrinite and liptinite (notably lamalginite and cutinite) are abundant in the maceral assemblages of both formations. Pristane/*n*-C<sub>17</sub> and phytane/*n*-C<sub>18</sub> ratios and C<sub>29</sub>-dominant sterane signatures also reflect the terrigenous source affinity of their organic matter.

Based on vitrinite reflectance, Rock–Eval  $T_{max}$ , *n*-alkane odd-over-even predominance, maturity-sensitive hopane ratios, and isomerization of C<sub>29</sub> steranes, both formations are thermally immature to early mature. Oil staining in the Murta Formation at two well localities proves that local oil generation and migration have occurred.

The source rock data obtained in this study are suitable for integration into existing numerical petroleum system models of the Cooper Basin (e.g. that of Hall and Palu 2016), in which the Eromanga Basin only represents overburden and its source rock properties are not yet taken into account. Finally, it would benefit the wider understanding of the Cooper/Eromanga petroleum province if our newly acquired data were to be incorporated in future oil-source correlation and lateral continuity studies.

**Supplementary Information** The online version contains supplementary material available at <https://doi.org/10.1007/s00531-022-02231-z>.

**Acknowledgements** We thank Mark Kelly, Chris Hansen, Bernadette Parkes and Alison Troup (Queensland Government; Department of Natural Resources, Mines and Energy; Exploration Data Centre) and we thank David Groom, Tony Hill and Jo Davies (Government of South Australia; South Australia Drill Core Reference Library) for support during core inspection and sampling. We also thank Associate Prof. David McKirdy (University of Adelaide) and Dr. Bernd Michaelsen (Geological Survey of South Australia) as well as Dr. Oliver Gaede and Dr. Scott Bryan (Queensland University of Technology) for very helpful discussions and sharing of useful literature and Dr. Paul Hackley (USGS) and Dr. Thomas Gentzis (Core Laboratories LP), who helped to improve an earlier draft of the manuscript. Further, we are thankful for the logistic and scientific support from our colleagues and

the laboratory staff at the Institute of Geology and Geochemistry of Petroleum and Coal (RWTH Aachen University): Louisa Helm, Donka Macherey, Kerstin Windeck and Dr. Laura Zieger. Further, we thank reviewers Associate Prof. David McKirdy and Dr. Robert Tscherny for their detailed and constructive reviews of this paper. Finally, JR is very grateful for additional funding by VAG (Vereinigung Aachener Geowissenschaftler e.V.) and the steady support of Prof. Dr. Dietrich Welte.

**Author contributions** JR: conceptualization, investigation, sample acquisition, data acquisition & curation, visualization, writing—original draft preparation. AB: methodology, validation. FF: investigation. JO: investigation. CB: supervision, validation, writing—review & editing. LH: supervision. RL: funding acquisition, project administration, supervision, validation, writing—review & editing.

**Funding** Open Access funding enabled and organized by Projekt DEAL. The field trip to Australia in August 2018 for core inspection and sampling was funded by the Vereinigung Aachener Geowissenschaftler (VAG e.V.).

**Availability of data and material** All obtained data during this study are given in this article and in the corresponding supplemental material. Polished sections of the analysed samples are available on request.

**Code availability** There was no code or software generated during this study.

## Declarations

**Conflict of interest** The authors declare that they have no known competing financial interests or personal relationships that could have appeared to influence the work reported in this paper.

**Ethics approval** Does not apply.

**Consent to participate** Does not apply.

**Consent for publication** Does not apply.

**Open Access** This article is licensed under a Creative Commons Attribution 4.0 International License, which permits use, sharing, adaptation, distribution and reproduction in any medium or format, as long as you give appropriate credit to the original author(s) and the source, provide a link to the Creative Commons licence, and indicate if changes were made. The images or other third party material in this article are included in the article's Creative Commons licence, unless indicated otherwise in a credit line to the material. If material is not included in the article's Creative Commons licence and your intended use is not permitted by statutory regulation or exceeds the permitted use, you will need to obtain permission directly from the copyright holder. To view a copy of this licence, visit <http://creativecommons.org/licenses/by/4.0/>.

## References

- Alberdi M, Moldowan JM, Peters KE, Dahl JE (2001) Stereoselective biodegradation of tricyclic terpanes in heavy oils from the Bolivar Coastal Fields, Venezuela. *Organic Geochem* 32(1):181–191
- Alexander EM, Sansome A (1996) Lithostratigraphy and environments of deposition. In: Alexander EM, Hibburt JE (eds) *The petroleum geology of South Australia*. Vol. 2: Eromanga Basin, Report Book 96/20. Department of Mines and Energy South Australia, pp 101–110
- Alexander EM, Sansome A, Cotton TB (2006) Lithostratigraphy and environments of deposition. In: Cotton TB, Scardigno MF, Hibburt JE (eds) *Petroleum Geology of South Australia Series*. The petroleum geology of South Australia, vol. 2: Eromanga Basin (2nd edn), Department of Primary Industries and Resources, South Australia
- Ambrose G, Suttill R, Lavering I (1986) The geology and hydrocarbon potential of the Murta Member (Mooga Formation) in the Southern Eromanga Basin. *Contributions to the Geology and Hydrocarbon Potential of the Eromanga Basin*. *Geol Soc Aust Spec Publ* 12:71–84
- Ambrose G, Suttill R, Lavering I (1982) A review of the Early Cretaceous Murta Member in the southern Eromanga Basin. In: *Eromanga Basin Symposium* (1982). Petroleum Exploration Society of Australia (PESA)
- Apak SN, Stuart WJ, Lemon NM, Wood G (1997) Structural evolution of the permian-triassic cooper Basin, Australia: relation to hydrocarbon trap styles. *AAPG Bull* 81(4):533–555
- Australian Petroleum Production & Exploration Association, APPEA (2020) APPEA Annual Production Statistics 2013. [http://www.appea.com.au/?attachment\\_id=5432](http://www.appea.com.au/?attachment_id=5432). Accessed 07 Feb 2020
- Arouri KR, McKirdy DM, Schwark L, Leythaeuser D, Boulton PJ (2004) Accumulation and mixing of hydrocarbons in oil fields along the Murteree Ridge, Eromanga Basin, South Australia. *Organic Geochem* 35(11–12):1597–1618
- Australian Government, Bioregional Assessment, AGBA (2013) Australian geological provinces (vol 2, 2013.01 ed., scale 1:2,500,000). Bioregional Assessment Source Dataset. Geoscience Australia, Canberra, Australia. <http://data.bioregionalassessments.gov.au/dataset/13ad6933-ee80-4c51-a97b-bac1e8bef16d>. Accessed 22 Apr 2020
- Australian Government, Bioregional Assessment, AGBA (2015) Stratigraphy of the Cooper subregion, showing geological ages, units, rock types and basin associations. <https://www.bioregionalassessments.gov.au/assessments/11-context-statement-cooper-subregion/1132-stratigraphy-and-rock-type>. Accessed 22 Apr 2020
- Australian Government, Geoscience Australia, GA (2020a) Great Artesian Basin. <http://www.ga.gov.au/scientific-topics/water/groundwater/gab>. Accessed 22 Apr 2020a
- Australian Government, Geoscience Australia, GA (2020b). Australian Stratigraphic Units Database. <http://www.ga.gov.au/data-pubs/data-standards/reference-databases/stratigraphic-units>. Accessed 22 Apr 2020b
- Béhar F, Pelet R, Roucace J (1984) Geochemistry of asphaltenes. *Org Geochem* 6:587–595
- Berner RA (1984) Sedimentary pyrite formation: an update. *Geochim Cosmochim Acta* 48(4):605–615
- Berner RA, Raiswell R (1984) C/S method for distinguishing freshwater from marine sedimentary rocks. *Geology* 12(6):365–368
- Blumenberg M, Zink KG, Scheeder G, Ostertag-Henning C, Erbacher J (2019) Biomarker paleo-reconstruction of the German Wealden (Berriasian, Early Cretaceous) in the Lower Saxony Basin (LSB). *Int J Earth Sci* 108:229–244. <https://doi.org/10.1007/s00531-018-1651-5>
- Boreham CJ, Hill AJ (1998) Source rock distribution and hydrocarbon geochemistry. *Petrol Geol South Aust* 4:129–142
- Boreham CJ, Powell TG (1987) Sources and preservation of organic matter in the Cretaceous Toolebuc Formation, eastern Australia. *Org Geochem* 11(6):433–449
- Boreham CJ, Summons RE (1999) New insights into the active petroleum systems in the Cooper and Eromanga Basins, Australia. *APPEA J* 39(1):263–296

- Boreham CJ, Horsfield B, Schenk HJ (1999) Predicting the quantities of oil and gas generated from Australian Permian coals, Bowen Basin using pyrolytic methods. *Mar Pet Geol* 16(2):165–188
- Boult PJ (1993) Membrane seal and tertiary migration pathways in the Bodalla South oilfield, Eromanga Basin, Australia. *Mar Petrol Geol* 10(1):3–13
- Boult PJ, Ryan MJ, Michaelsen BH, McKirdy DM, Tingate PR, Lanzilli E, Kagya ML (1997) The Birkhead–Hutton (!) Petroleum System of the Gidgealpa Area, Eromanga Basin, Australia. In: Conference on petroleum systems of SE Asia and Australasia, 1997. Conference proceedings. Indonesian Petroleum Association, pp 213–236. <https://doi.org/10.29118/ipa.965.213.235>
- Bowering OJW (1982) Hydrodynamics and hydrocarbon migration—a model for the Eromanga Basin. *APPEA J* 22(1):227–236
- Bowering OJW, Harrison DM (1986) The Merrimelia oil and gas field—a case history. In: Gravestock DI, Moore PS, Pitt GM (eds) Contributions to the geology and hydrocarbon potential of the Eromanga basins: Geological Society of Australia Special Publication 12, pp 183–194
- Burger D (1986) Palynology, cyclic sedimentation, and palaeoenvironments in the Late Mesozoic of the Eromanga Basin. *Geol Soc Spec Pub* 12:53–70
- Carr LK, Korsch RJ, Palu TJ, Reese B (2016) Onshore basin inventory: the McArthur, South Nicholson, Georgina, Wiso, Amadeus, Warburton, Cooper and Galilee basins, central Australia. *Geoscience Australia Record* 2016/04. Geoscience Australia, Canberra
- Connan J, Cassou AM (1980) Properties of gases and petroleum liquids derived from terrestrial kerogen at various maturation levels. *Geochim Cosmochim Acta* 44(1):1–23
- Cook AG, Bryan SE, Draper J (2013) Post-orogenic Mesozoic basins and magmatism. In: Jell P (ed) *Geology of Queensland*. Geological Survey of Queensland, Australia, pp 515–575
- Deighton I, Hill AJ (1998) Thermal and burial history. *Petrol Geol S Aust* 4:143–155
- Deighton I, Draper JJ, Hill AJ, Boreham CJ (2003) A hydrocarbon generation model for the Cooper and Eromanga Basins. *APPEA J* 43(1):433–451
- Derenne S, Largeau C, Casadevall E, Connan J (1988) Comparison of torbanites of various origins and evolutionary stages. Bacterial contribution to their formation. Causes of the lack of botryococcane in bitumens. *Org Geochem* 12(1):43–59. [https://doi.org/10.1016/0146-6380\(88\)90114-3](https://doi.org/10.1016/0146-6380(88)90114-3)
- Draper JJ (2002) Queensland Minerals and Energy Review Series. *Geology of the Cooper and Eromanga Basins*, Queensland. Queensland Department of Natural Resources and Mines
- Espitalié J, Laporte JL, Madec M, Marquis F, Leplat P, Paulet J, Boutefeu A (1977) Rapid method for source rocks characterization and for determination of petroleum potential and degree of evolution. *Revue De L Institut Francais Du Petrole* 32(1):23–42
- Espitalié J, Deroo G, Marquis F (1985) La pyrolyse Rock-Eval et ses applications. Deuxième partie. *Revue de l'Institut français du Pétrole* 40(6):755–784
- Exon NF (1966) Revised Jurassic to Lower Cretaceous stratigraphy in the south-east Eromanga Basin, Queensland. *Qld Gov Min J* 67:232–238
- Fan P, King JD, Claypool GE (1987) Characteristics of biomarker compounds in Chinese crude oils. In: Kumar RK, Dwivedi P, Banerjee V, Gupta V (eds) *Petroleum geochemistry and exploration in the Afro-Asian Region*. Balkema, Rotterdam, pp 197–202
- Fang R, Littke R, Zieger L, Baniasad A, Li M, Schwarzbauer J (2019) Changes of composition and content of tricyclic terpane, hopane, sterane, and aromatic biomarkers throughout the oil window: a detailed study on maturity parameters of Lower Toarcian Posidonia Shale of the Hils Syncline, NW Germany. *Org Geochem* 138:103928
- Glikson M, Lindsay K, Saxby J (1989) Botryococcus—a planktonic green alga, the source of petroleum through the ages: transmission electron microscopical studies of oil shales and petroleum source rocks. *Org Geochem* 14(6):595–608
- Goldstein B, Menpes S, Hill A, Wickham A, Alexander E, Jarosz M, Pepicelli D, et al (2012) Roadmap for unconventional gas projects in South Australia: Adelaide, Australia. Department for Manufacturing, Innovation, Trade, Resources and Energy, Energy Resources Division
- Gorter JD (1994) Sequence stratigraphy and the depositional history of the Murta Member (upper Hooray Sandstone), southeastern Eromanga Basin, Australia: implications for the development of source and reservoir facies. *APPEA J* 34(1):644–673
- Gravestock DI, Gatehouse CG, Drexel JF, Preiss WV (1995) The Geology of South Australia (vol 2: The Phanerozoic. Cooper Basin)
- Gravestock DI, Hibbert J, Drexel JF (1998) *Petroleum Geology of South Australia (vol 4: Cooper Basin)*. Petroleum Group, Primary Industries and Resources SA
- Gray ARG, Draper JJ (2002) *Petroleum geology. Geology of the Cooper and Eromanga Basins*. Queensland Department of Natural Resources and Mines, Brisbane, Australia, pp 63–74
- Greenstreet C, Dello L (2015) Santos and the Cooper Basin: the next frontier. *Gas Today* 32:76–78
- Guo Q, Littke R, Sun Y, Zieger L (2020) Depositional history of low-maturity coals from the Puyang Basin, Yunnan Province, China. *Int J Coal Geol* 221:103428
- Hackley PC, Cardott BJ (2016) Application of organic petrography in North American shale petroleum systems: a review. *Int J Coal Geol* 163:8–51
- Hackley PC, Dennen KO, Garza D, Lohr CD, Valentine BJ, Hatcherian JJ et al (2020) Oil-source rock correlation studies in the unconventional Upper Cretaceous Tuscaloosa marine shale (TMS) petroleum system, Mississippi and Louisiana, USA. *J Petrol Sci Eng* 190:107015
- Hall LS, Hill T, Wang L, Edwards D, Kuske T, Troup A, Boreham CJ (2015) Unconventional gas prospectivity of the Cooper Basin. *APPEA J* 55(2):428–428
- Hall LS, Palu TJ, Murray AP, Boreham CJ, Edwards DS, Hill AJ, Troup A (2019) Hydrocarbon prospectivity of the Cooper Basin, Australia. *AAPG Bull* 103(1):31–63
- Hall LS, Palu TJ (2016) Cooper Basin regional petroleum systems model. Geoscience Australia, Canberra. <http://pid.geoscience.gov.au/dataset/ga/100740>. Accessed 03 Nov 2020
- Hall LS, Hill AJ, Troup A, Korsch RJ, Radke BM, Nicoll RS, Palu TJ, Wang L, Stacey A (2016) Cooper Basin architecture and lithofacies. Regional hydrocarbon prospectivity of the Cooper Basin (Part 1, Geoscience Australia Record: 2015/31). Geoscience Australia, Canberra
- Hallmann COE, Arouri KR, McKirdy DM, Schwark L (2006) A new perspective on exploring the Cooper/Eromanga petroleum province—evidence of oil charging from the Warburton basin. *APPEA J* 46(1):261–282
- Hartkopf-Fröder C, Königshof P, Littke R, Schwarzbauer J (2015) Optical thermal maturity parameters and organic geochemical alteration at low grade diagenesis to anchimetamorphism: a review. *Int J Coal Geol* 150:74–119
- Hawkins PJ, Almond CS, Carmichael DC, Smith RJ, Williams LJ (1989) Kerogen Characterisation, and Organic and Mineral Diagenesis of Potential Source Rocks in Jurassic Units, Southern Eromanga Basin, Queensland. In: Proceedings of the Cooper and Eromanga Basins Conference (1989). Petroleum Exploration Society of Australia (PESA)
- Hedges JL, Eglinton G, Hatcher PG, Kirchner DL, Arnosti C, Derenne S et al (2000) The molecularly-uncharacterized component of nonliving organic matter in natural environments. *Org Geochem* 31(10):945–958

- Huang W-Y, Meinschein WG (1979) Sterols as ecological indicators. *Geochim Cosmochim Acta* 43(5):739–745. [https://doi.org/10.1016/0016-7037\(79\)90257-6](https://doi.org/10.1016/0016-7037(79)90257-6)
- Hughes WB, Holba AG, Dzou LIP (1995) The ratios of dibenzothio-*phene* to phenanthrene and pristane to phytane as indicators of depositional environment and lithology of petroleum source rocks. *Geochim Cosmochim Acta* 59(17):3581–3598
- Hunt JM (1996) *Petroleum geochemistry and geology*, 2nd edn. Freeman and Company, New York
- Jadoon QK, Roberts E, Blenkinsop T, Wust R (2016) Organic petrography and thermal maturity of the Permian Roseneath and Murteree shales in the Cooper Basin, Australia. *Int J Coal Geol* 154:240–256
- Jarvie DM (2012) Shale resource systems for oil and gas: Part 2—Shale-oil resource systems. In: Breyer JA (ed) *Shale reservoirs—giant resources for the 21st century: AAPG Memoir*, vol 97, pp 89–119
- Jenkins CC (1989) Geochemical correlation of source rocks and crude oils from the Cooper and Eromanga Basins. In: *Proceedings of the Cooper and Eromanga Basins Conference 1989*. Petroleum Exploration Society of Australia (PESA)
- Kagya MLN (1997) The source rock and petroleum geochemistry of the Early Jurassic Poolowanna Formation, Eromanga Basin. PhD thesis, University of Adelaide, Australia
- Khorasani GK (1987) Recent organic geochemical evaluation of the central Eromanga basin. *APPEA J* 27(1):106–111
- Langford FF, Blanc-Valleron MM (1990) Interpreting Rock-Eval pyrolysis data using graphs of pyrolyzable hydrocarbons vs. total organic carbon. *AAPG Bull* 74(6):799–804
- Lanzilli E (1999) The Birkhead Formation: reservoir characterisation of the Gidgealpa south dome and sequence stratigraphy of the Eromanga Basin, Australia. Doctoral dissertation, University of Adelaide, Australia
- Law CA (1999) Chapter 6—evaluating source rocks. In: Beaumont EA, Foster NH (eds) *Treatise of petroleum geology/handbook of petroleum geology: exploring for oil and gas traps* (1st edn). AAPG. ISBN 978-1-58861-493-3
- Lijmbach GWM (1975) On the origin of petroleum. In: *Proceedings of the 9th World Petroleum Congress*, vol 1. Applied Sciences Publisher, Special Paper, Tokyo. London, pp 357–369. <https://www.onepetro.org/conference-paper/WPC-16134>. Accessed 03 Nov 2020
- Mackie SI, Gumley CM (1995) The Dirkala South oil discovery: focussing on cost-efficient reservoir delineation. *APPEA J* 35(1):65–78
- Mahlstedt N, Horsfield B (2016) Source rock evaluation and predicted petroleum compositions related to samples from the Adavale, Bowen, Cooper and Eromanga Basins, Queensland. *GEOS4 REPORT 20161216 (ROUND 2)*. QDEX Report number CR 99555. Department of Natural Resources and Mines, Queensland, Australia. [https://qdexguest.dnrm.qld.gov.au/portal/site/qdex/search?REPORT\\_ID=99555&COLLECTION\\_ID=999](https://qdexguest.dnrm.qld.gov.au/portal/site/qdex/search?REPORT_ID=99555&COLLECTION_ID=999). Accessed 08 Feb 2020
- Maslen E, Grice K, Métayer PL, Dawson D, Edwards D (2011) Stable carbon isotopic compositions of individual aromatic hydrocarbons as source and age indicators in oils from western Australian basins. *Org Geochem* 42(4):387–398. <https://doi.org/10.1016/j.orggeochem.2011.02.005>
- McIntyre SM, Jamal FG, Pidcock CL, Kabir MI (1989) The Gidgealpa oil and gas field: a case history. In: O'Neil BJ (ed) *The Cooper & Eromanga Basins, Australia (Proceedings of the Cooper and Eromanga Basins Conference, 1989)*. Petroleum Exploration Society of Australia (PESA)
- McKirdy DM, Cox RE, Volkman JK, Howell VJ (1986a) Botryococane in a new class of Australian non-marine crude oils. *Nature* 320(6057):57–59
- McKirdy DM, Emmett JK, Mooney BA, Cox RE, Watson BL (1986b) Organic geochemical facies of the Cretaceous Bulldog Shale, western Eromanga Basin, South Australia. In: Gravestock DI, Moore PS, Pitt GM (eds) *Contributions to the geology and hydrocarbon potential of the Eromanga Basin (Special Publication, 12:287–304)*. Geological Society of Australia
- McKirdy DM, Michaelsen BH, Kagya MLN, Ryan MJ (1997) Biomarker signatures of oils from the Patchawarra Trough, Cooper/Eromanga Basin, South Australia. In: 18th International Meeting on Organic Geochemistry Abstracts (18th IMOG). Maastricht, The Netherlands, pp 415–416
- McKirdy DM, Yu X, Leythaeuser D, Schwark L, Arouri KR (2001) A pilot study of secondary migration and reservoir filling in the Cooper/Eromanga Basin, South Australia. In: 20th International Meeting on Organic Geochemistry Abstracts (20th IMOG). Nancy, France, pp 425–426
- Menpes S, Hill A, Pepicelli D (2013) Characteristics of the Gidgealpa Group composite resource play in the Cooper Basin, South Australia. In: *Unconventional Resources Technology Conference Abstracts*. SEG Society of Exploration Geophysicists, AAPG American Association of Petroleum Geologists, SPE Society of Petroleum Engineers, pp 2621–2630
- Metzger P, Largeau C (2005) *Botryococcus braunii*: a rich source for hydrocarbons and related ether lipids. *Appl Microbiol Biotechnol* 66:486–496. <https://doi.org/10.1007/s00253-004-1779-z>
- Michaelsen BH (2002) Geochemical perspectives on the petroleum habitat of the Cooper and Eromanga Basins, central Australia (Doctoral dissertation). University of Adelaide, Australia
- Michaelsen BH, McKirdy DM (1989) Organic facies and petroleum geochemistry of the lacustrine Murta Member (Mooga Formation) in the Eromanga Basin, Australia. In: O'Neil BJ (ed) *The Cooper & Eromanga Basins, Australia (Proceedings of the Cooper and Eromanga Basins Conference, 1989)*. Petroleum Exploration Society of Australia (PESA)
- Michaelsen BH, McKirdy DM (2001) Migration and mixing of oils in the Cooper and Eromanga Basins, Central Australia. In: Hill KC, Bernecker T (eds) *Eastern Australian Basins Symposium 2001*. (Petroleum Exploration Society of Australia Special Publication). Petroleum Exploration Society of Australia, Melbourne, Australia, pp 289–300
- Michaelsen BH, McKirdy DM (2006) Source rock distribution and hydrocarbon geochemistry. In: Cotton TB, Scardigno MF, Highburt JE (eds) *Petroleum Geology of South Australia Series. The petroleum geology of South Australia (Vol. 2: Eromanga Basin (2nd ed.))*. Department of Primary Industries and Resources, South Australia
- Moldowan JM, Seifert WK (1980) First discovery of botryococane in petroleum. *J Chem Soc, Chem Commun* 19:912–914
- Moldowan JM, Seifert WK, Gallegos EJ (1983) Identification of an extended series of tricyclic terpanes in petroleum. *Geochim Cosmochim Acta* 47(8):1531–1534
- Moldowan JM, Seifert WK, Gallegos EJ (1985) Relationship between petroleum composition and depositional environment of petroleum source rocks. *AAPG Bull* 69(8):1255–1268
- Moldowan JM, Dahl J, Huizinga BJ, Fago FJ, Hickey LJ, Peakman TM, Taylor DW (1994) The molecular fossil record of oleanane and its relation to angiosperms. *Science* 265(5173):768–771. <https://doi.org/10.1126/science.265.5173.768>
- Moore P, Hobday D, Mai H, Sun Z (1986) Comparison of selected non-marine petroleum-bearing basins in Australia and China. *APEA J* 26(1):285–309
- Mount TJ (1981) Dullingari North 1, an oil discovery in the Murta Member of the Eromanga Basin. *APEA J* 21(1):71–77
- Mount TJ (1982) Geology of the Dullingari Murta oilfield. In: *Eromanga Basin Symposium (1982)*. Petroleum Exploration Society of Australia (PESA)

- O'Neil BJ, Alexander EM (2006) History of petroleum exploration and development. In: Cotton TB, Scardigno MF, Hibburt JE (eds) *Petroleum Geology of South Australia Series. The petroleum geology of South Australia, vol. 2: Eromanga Basin* (2nd ed.). South Australia. Department of Primary Industries and Resources
- O'Neil BJ (1998) Chapter 2: history of petroleum exploration and development. In: Gravestock DI, Hibburt JE, Drexel JF (eds) *The Petroleum Geology of South Australia. Volume 4: Cooper Basin*. South Australia Department of Primary Industries and Resources, Adelaide. Report Book, 1998/9, 7–36. <https://sarig.basis.pir.sa.gov.au/WebtopEw/ws/samref/sarig1/image/DDD/PGSA004.pdf>. Accessed 03 Nov 2020
- Ouriisson G, Albrecht P, Rohmer M (1982) Predictive microbial biochemistry—from molecular fossils to procaryotic membranes. *Trends Biochem Sci* 7(7):236–239
- Paton IM (1986) Contributions to the geology and hydrocarbon potential of the eromanga Basin. *Geol Soc Aust Spec Publ* 12:195–201
- Peters KE (1986) Guidelines for evaluating petroleum source rock using programmed pyrolysis. *AAPG Bull* 70(3):318–329
- Peters KE, Fraser TH, Amris W, Rustanto B, Hermanto E (1999) *Geochemistry of crude oils from eastern Indonesia*. AAPG Bull 83(12):1927–1942
- Peters KE, Cassa MR (1994) Applied source rock geochemistry: Chapter 5: part II. Essential elements. In: Magoon LB, Dow WG (eds) *The petroleum system—from source to trap*. AAPG Memoir 60
- Peters KE, Walters CC, Moldowan JM (2005a) *The Biomarker Guide, Volume 1: biomarkers and isotopes in the environment and human history* (2nd edn). Cambridge University Press, New York. ISBN 0521781582, <https://doi.org/10.1017/CBO9780511524868>
- Peters KE, Walters CC, Moldowan JM (2005b) *The biomarker guide, vol 2: biomarkers and isotopes in petroleum exploration and earth history* (2nd edn). Cambridge University Press, New York. ISBN 0521837626, <https://doi.org/10.1017/CBO9781107326040>
- Powell TG (1986) Petroleum geochemistry and depositional setting of lacustrine source rocks. *Mar Pet Geol* 3(3):200–219
- Powell TG, Boreham CJ, McKirdy DM, Michaelsen BH, Summons RE (1989) Petroleum geochemistry of the Murta Member, Mooga Formation, and associated oils, Eromanga Basin. *APPEA J* 29(1):114–129
- Powell TG, Boreham CJ, Smyth M, Russell N, Cook AC (1991) Petroleum source rock assessment in non-marine sequences: pyrolysis and petrographic analysis of Australian coals and carbonaceous shales. *Org Geochem* 17(3):375–394
- QLD Ref. No. 27146 = Local referencenumber of the sampled core material at the drill core reference library in Brisbane, Queensland. <https://www.business.qld.gov.au/industries/mining-energy-water/resources/geoscience-information/exploration-incentives/drillcore>. Accessed 13 Aug 2022
- Radke M, Welte DH, Willsch H (1982) Geochemical study on a well in the Western Canada Basin: relation of the aromatic distribution pattern to maturity of organic matter. *Geochim Cosmochim Acta* 46(1):1–10. [https://doi.org/10.1016/0016-7037\(82\)90285-X](https://doi.org/10.1016/0016-7037(82)90285-X)
- Reeves F (1947) *Geology of Roma District, Queensland, Australia*. AAPG Bull 31(8):1341–1371
- Röth J, Littke R (2022) Down under and under cover—the tectonic and thermal history of the cooper and central Eromanga Basins (Central Eastern Australia). *Geosciences* 2022(12):117. <https://doi.org/10.3390/geosciences12030117>
- SA Ref. No. 4857 = Local reference number of the sampled core material at the drill core referencelibrary in Adelaide, South Australia. [https://energymining.sa.gov.au/minerals/geoscience/drill\\_core\\_reference\\_library](https://energymining.sa.gov.au/minerals/geoscience/drill_core_reference_library). Accessed 13 Aug 2022
- Salomon JA, Keenihan SL, Calcraft AP (1990) Bodalla South Field. In: Salomon JA, Keenihan SL, Calcraft AP (eds) *TR: Structural Traps I: Tectonic Fold Traps* (AAPG Special Volumes). American Association of Petroleum Geologists, pp 129–155
- Sawlowicz Z (1993) Pyrite framboids and their development: a new conceptual mechanism. *Geol Rundsch* 82:148–156. <https://doi.org/10.1007/BF00563277>
- Scalan ES, Smith JE (1970) An improved measure of the odd-even predominance in the normal alkanes of sediment extracts and petroleum. *Geochim Cosmochim Acta* 34(5):611–620. [https://doi.org/10.1016/0016-7037\(70\)90019-0](https://doi.org/10.1016/0016-7037(70)90019-0)
- Scheidt G, Littke R (1989) Comparative organic petrology of inter-layered sandstones, siltstones, mudstones and coals in the Upper Carboniferous Ruhr basin, Northwest Germany, and their thermal history and methane generation. *Geol Rundsch* 78(1):375–390
- Schulz-Rojahn JP (1993) Calcite-cemented zones in the Eromanga Basin: clues to petroleum migration and entrapment? *APPEA J* 33(1):63–76. <https://doi.org/10.1071/AJ92006>
- Schwarzbauer J, Jovančičević B (2020) Principal analytical procedures in organic geochemistry. Introduction to analytical methods in organic geochemistry. Springer, Cham, pp 135–145
- Seifert WK, Moldowan JM (1980) The effect of thermal stress on source-rock quality as measured by hopane stereochemistry. *Phys Chem Earth* 12:229–237. [https://doi.org/10.1016/0079-1946\(79\)90107-1](https://doi.org/10.1016/0079-1946(79)90107-1)
- Seifert WK, Moldowan JM (1986) Use of biological markers in petroleum exploration. In: Johns RB (ed) *Method in geochemistry and geophysics*, vol 24. Elsevier, Amsterdam, pp 261–290
- Seifert WK, Moldowan JM, Jones RW (1981) Application of biologic markers in combination with stable carbon isotopes to source rock/oil correlations, Prudhoe Bay, Alaska. *AAPG Bull* 65(5):990–991
- Sinninghe Damsté JS, Kenig F, Koopmans MP, Koster J, Schouten S, Hayes JM, de Leeuw JW (1995) Evidence for gammacerane as an indicator of water column stratification. *Geochim Cosmochim Acta* 59(9):1895–1900
- Smerdon BD, Ransley TR, Radke BM, Kellett JR (2012) Water resource assessment for the Great Artesian Basin. A report to the Australian government from the CSIRO Great Artesian Basin water resource assessment. CSIRO Water for a Healthy Country Flagship, Australia. Australian Government
- Taylor GH, Teichmüller M, Davis A, Diessel CFK, Littke R, Robert P (1998) *Organic petrology*. Gebrüder Borntraeger, Berlin. <https://doi.org/10.1017/S001675689946332>
- ten Haven HL, Rullkötter J (1988) The diagenetic fate of taraxer-14-ene and oleanene isomers. *Geochim Cosmochim Acta* 52:2543–2548
- Tissot BP, Welte DH (1984) From kerogen to petroleum. In: Tissot BP, Welte DH (eds) *Petroleum formation and occurrence*. Springer, Berlin, Heidelberg, pp 160–198
- van Aarssen BG, Bastow TP, Alexander R, Kagi RI (1999) Distributions of methylated naphthalenes in crude oils: indicators of maturity, biodegradation and mixing. *Org Geochem* 30(10):1213–1227. [https://doi.org/10.1016/S0146-6380\(99\)00097-2](https://doi.org/10.1016/S0146-6380(99)00097-2)
- Veevers JJ (1984) *Phanerozoic earth history of Australia*. Oxford University Press, ISBN, p 0198544596
- Veevers JJ, Powell CM, Roots SR (1991) Review of seafloor spreading around Australia I Synthesis of the patterns of spreading. *Aust J Earth Sci* 38(4):373–389
- Vincent PW, Mortimore IR, McKirdy DM (1985) Hydrocarbon generation, migration and entrapment in the Jackson-Naccowlah area, ATP 259P, Southwestern Queensland. *APPEA J* 25(1):62–84
- Wainman CC, McCabe PJ, Crowley JL (2018) Solving a tuff problem: defining a chronostratigraphic framework for Middle to Upper Jurassic nonmarine strata in eastern Australia using

- uranium—lead chemical abrasion—thermal ionization mass spectrometry zircon dates. *AAPG Bull* 102(6):1141–1168
- Watts KJ (1987) The Hutton Sandstone-Birkhead Formation transition, ATP 269P (1), Eromanga Basin. *APPEA J* 27(1):215–229
- Wecker HRB (1989) The Eromanga Basin. *APPEA J* 29(1):379–397
- Yang S, Horsfield B (2020) Critical review of the uncertainty of Tmax in revealing the thermal maturity of organic matter in sedimentary rocks. *Int J Coal Geol* 103500
- Zieger L, Littke R (2019) Bolsovian (Pennsylvanian) tropical peat depositional environments: the example of the Ruhr Basin, Germany. *Int J Coal Geol* 211:103209
- Ziegs V, Mahlstedt N, Bruns B, Horsfield B (2015) Predicted bulk composition of petroleum generated by Lower Cretaceous Wealden black shales, Lower Saxony Basin, Germany. *Int J Earth Sci* 104(6):1605–1621
- Zoellner E (1988) Geology of the Early Cretaceous Murta Member (Mooga Formation) in the Cooper Basin area, South Australia and Queensland. Doctoral dissertation. Flinders University of South Australia
- Zumberge JE (1987) Terpenoid biomarker distributions in low maturity crude oils. *Org Geochem* 11:479–496